

A numerical investigation on the suspended sediment dynamics and sediment budget in the Mekong Delta

Thanh, Vo Quoc; Roelvink, Dano; van der Wegen, Mick; Reynolds, Johan; van der Spek, Ad; Van Vinh, Giap; Phuong Linh, Vo Thi; Tu, Le Xuan; Trung, Nguyen Hieu

DOI

[10.1016/j.csr.2025.105427](https://doi.org/10.1016/j.csr.2025.105427)

Publication date

2025

Document Version

Final published version

Published in

Continental Shelf Research

Citation (APA)

Thanh, V. Q., Roelvink, D., van der Wegen, M., Reynolds, J., van der Spek, A., Van Vinh, G., Phuong Linh, V. T., Tu, L. X., & Trung, N. H. (2025). A numerical investigation on the suspended sediment dynamics and sediment budget in the Mekong Delta. *Continental Shelf Research*, 286, Article 105427. <https://doi.org/10.1016/j.csr.2025.105427>

Important note

To cite this publication, please use the final published version (if applicable). Please check the document version above.

Copyright

Other than for strictly personal use, it is not permitted to download, forward or distribute the text or part of it, without the consent of the author(s) and/or copyright holder(s), unless the work is under an open content license such as Creative Commons.

Takedown policy

Please contact us and provide details if you believe this document breaches copyrights. We will remove access to the work immediately and investigate your claim.



A numerical investigation on the suspended sediment dynamics and sediment budget in the Mekong Delta

Vo Quoc Thanh^{a,b,c,*}, Dano Roelvink^{a,b,d}, Mick van der Wegen^{a,d}, Johan Reyns^{a,d},
Ad van der Spek^d, Giap Van Vinh^e, Vo Thi Phuong Linh^c, Le Xuan Tu^f, Nguyen Hieu Trung^g

^a Department of Water Science and Engineering, IHE Delft, Delft, the Netherlands

^b Faculty of Civil Engineering and Geosciences, Delft University of Technology, Delft, the Netherlands

^c College of Environment and Natural Resources, Can Tho University, Can Tho, Viet Nam

^d Deltares, Delft, the Netherlands

^e Cui Long River Hydrological Center, Southern Regional Hydro-Meteorological Center, Can Tho, Viet Nam

^f The Southern Institute of Water Resources Research, Ho Chi Minh City, Viet Nam

^g Research Institute for Climate Change, Can Tho University, Can Tho, Viet Nam

ARTICLE INFO

Keywords:

Mekong delta
Mekong river
Delft3D-FM
Sediment budget
Hysteresis

ABSTRACT

Fluvial sediment supply towards the coast has been the subject of extensive research. Important aspects relate to the impact of sediment retaining hydropower dams, potential delta progradation, coastal sediment supply and delta vulnerability to sea level rise. Once validated, process-based models provide a valuable tool to address these aspects and offer detailed information on sediment pathways, distribution and budget in specific systems.

This study aims to advance the understanding of the sediment dynamics and sediment budget in the Mekong Delta system. We developed a process-based model (Delft3D FM) that allows for coupling 2D area grids to 1D network grids. The flexible mesh describes both wide river sections and channel irrigation and drainage networks present in the Mekong Delta. We calibrated the model against observed discharge, salinity, suspended sediment concentration (SSC) and sediment flux.

The model was able to skillfully describe seasonal variations of SSC and hysteresis of SSC and water discharge caused by the Tonle Sap Lake induced flow patterns and seasonally varying bed sediment availability in the channels. Model results suggest that the Mekong River delivers an amount of sediment, towards the delta which is much lower than the common estimate of 160 Mt/year. About 23% of the modeled total sediment load at Kratie reaches the sea. Our modeling approach is a useful tool to assess sediment dynamics under strategic anthropogenic interventions or climate change scenarios.

1. Introduction

The worldwide fluvial sediment flux to coastal deltas amounts to 12.8–15.1 Gt per year (Syvitski and Kettner, 2011). Understanding sedimentary processes in these deltas is important to estimate the impact of anthropogenic strategies for sustainable management and to address the impact of climate change like changing river flow, sediment supply, and sea-level rise. Sediment fluxes are commonly estimated in relation to river discharge (Ogston et al., 2017), but this is associated with high uncertainties due to sparse data, both in time and space. Tidal influence makes sediment dynamics in deltas even more complex to understand, while local conditions make every Delta unique.

The Mekong Delta is crucial to the local livelihoods and food security. The area is home to about 17 million people in the Vietnamese Mekong Delta (VMD) (Vo, 2012). Particularly, the VMD is a “rice bowl” for Vietnam and the world. The VMD covers a region of 39,700 km² and ~60% of this area is for agricultural cultivation (Vo, 2012). One of the important factors favoring agricultural cultivation is the abundant availability of water and sediment from the Mekong River. Annually, the Mekong River supplies ~416 km³ of water and delivers ~73 Mt sediment towards its Delta (Koehnken, 2014; MRC, 2005; Thanh et al., 2020a). The annual sediment transport at Kratie (Cambodia) varies in a range of 44–98 Mt/y from 2009 to 2013. These values fell within long-term estimates (87.4 ± 28.7 Mt/y) of Darby et al. (2016). Recent

* Corresponding author. Department of Water Science and Engineering, IHE Delft, Delft, the Netherlands.

E-mail address: quocthanh@ctu.edu.vn (V.Q. Thanh).

<https://doi.org/10.1016/j.csr.2025.105427>

Received 27 August 2023; Received in revised form 8 November 2024; Accepted 27 January 2025

Available online 29 January 2025

0278-4343/© 2025 Elsevier Ltd. All rights reserved, including those for text and data mining, AI training, and similar technologies.

studies (e.g. Darby et al., 2016; Kummur and Varis, 2007; Lu et al., 2014; Manh et al., 2014) confirmed that the suspended sediment flux into the Mekong Delta (at Kratie station) is much less than the commonly used value of 160 Mt/y. However, prior to the construction of hydropower dams on the Mekong River mainstream, sediment loads could have been substantially higher than afterward. The hydropower dams not only change the seasonal flows but also store sediment in their reservoirs. Lauri et al. (2012) found that these reservoirs can increase flows at Kratie in the low flow season by 25–160% and decrease flows in the high flow season by 24%. Annual floods are the main source of fresh water in the VMD while the sediments delivered act as a natural and valuable fertilizer source for agricultural crops (Chapman and Darby, 2016). However, the VMD is facing challenges related to flood regimes and sediment transport due to climate change, sea-level rise, and human interventions.

Sediment transport in the Mekong River has been estimated by *in-situ* measurements, sediment rating curve methods; and numerical modeling. Sediment measurements in the Mekong started in the 1960s, inspired by US practices (Walling, 2009). When using data-based methods, the reliability of sediment transport depends on the number of measuring stations, the length of records and the temporal resolution of the data. It has been hardly possible to cover a large area like the Mekong Delta with measurements. In addition, discontinuous records and low sampling frequency lead to high uncertainties in sediment budget estimations. A numerical model, calibrated by *in-situ* measurements and rating curves, is a suitable tool to investigate hydrodynamics and sediment transport in the Mekong Delta in more detail.

There exist a large number of studies focusing on sediment dynamics in the VMD, ranging from measurement-based studies to numerical modeling studies. Hung et al. (2014), Manh et al. (2013), and Nowacki et al. (2015) provide *in-situ* measurements on a limited number of locations in the VMD. The data of *in-situ* measurement are accurate, but it is difficult to collect them on a large spatial scale to derive sediment budgets on the scale of the entire VMD. However, *in-situ* measurement data are essential to calibrate and validate numerical models.

Numerical models for the entire Mekong Delta are commonly set up using a 1D schematization (Manh et al., 2014), while smaller-scale area models are represented by 2DH or 3D setups (Marchesiello et al., 2019; Thanh et al., 2017; Tu et al., 2019; Xing et al., 2017). For example, Thanh et al. (2017) and Tu et al. (2019) used a 3D, process-based model (Delft3D4) to investigate sediment dynamics and morphological changes in the coastal area of the Mekong Delta. With a similar approach, Xing et al. (2017) developed a model for the lower Song Hau channel to advance the understanding of hydrodynamics and sand transport in this region. Both the studies of Thanh et al. and Xing et al. used two spatial scales for modeling, including a large and coarse grid to act as boundary conditions for a fine and detailed grid. The use of this approach can reduce the computational cost, but it may cause significant uncertainties. Therefore, creating a single model domain for the entire Mekong Delta and its shelf could result in accurate results. A large part of the Mekong Delta consists of a dense channel network, with high variability in channel widths, which can be approached by a 1D network. A pure 2D model for the entire Mekong Delta would be unnecessary and computationally inefficient. 3D effects like gravitational circulation could be relevant only in more seaward reaches. In this study, we propose a 1D-2D coupled model for the Mekong Delta and shelf. The main channels of the Mekong River and floodplains are modeled in 2D while primary and secondary channels are represented by 1D elements. This approach was efficient for large-scale and complex regions and it accurately modeled hydrodynamics in the whole Mekong Delta (Thanh et al., 2020a).

The objective of this paper is to derive a sediment budget for the Vietnamese Mekong Delta for the high river flow year of 2011 using a 1D-2D coupled, process-based model (Delft3D Flexible Mesh, DFM). In section 2 we will introduce the Mekong Delta and its sediment characteristics. In section 3 we first describe the model DFM and the modeling

approach for the Mekong Delta. In section 4, the model calibration is presented, and we investigate sediment dynamics and estimate a sediment budget in the Mekong Delta. Finally, section 5 presents conclusions.

2. Case study description: The Mekong Delta

2.1. Characterization of the Mekong Delta

The Mekong Delta is the third largest delta in the world (Anthony et al., 2015). It has been formed over 6000 years ago in response to decelerating sea level rise (Mekong River Commission, 2010). The Mekong River is one of the world's largest rivers, with a length of approximately 4800 km and its draining catchment area of 795,000 km² (MRC, 2005). It flows through the six countries, originating from China, through Myanmar, Laos, Thailand, Cambodia, and Vietnam, before debouching into the East Sea (South China Sea). The Mekong Delta is commonly defined from Phnom Penh downstream, where the Mekong river is separated into two branches, namely Mekong and Bassac (Gupta and Liew, 2007; Renaud et al., 2013). The delta is located in Cambodia and Vietnam. The Mekong Delta in Cambodia (CMD) and Vietnam (VMD) have different hydrological regimes. An important confluence of the Mekong River and the Tonle Sap River, located at Phnom Penh, is responsible for this. During the initial phase of annual floods (July–October), the Mekong River also fills the Tonle Sap Lake via the Tonle Sap River. At decreasing flood flows, the lake empties again via the Tonle Sap River into the Mekong River. The lake thus lowers and elongates yearly hydrographs. In order to understand hydrodynamics and sediment dynamics in the Mekong Delta, extending the area up to Kratie (Fig. 1) is needed (Thanh et al., 2017).

The CMD encompasses a large area of lowland which is deeply inundated by the annual floods. For instance, inundation depths on the CMD floodplains are generally over 3 m (Fujii et al., 2003). The hydrodynamics of the Mekong River in the CMD is dominated by the annual floods which are considerably changed due to the southwest monsoon (Yu et al., 2018). In addition, the hydrodynamics in this region are also influenced by the regulation of the Tonle Sap Lake.

The VMD has a complex river network that contains a large number of man-made canals. Extensive canal development for agricultural purposes started in 1819 (Hung, 2011) and is growing presently. Seventy-five percent of the VMD area is used for agricultural production (Kakonen, 2008). Recently, several hydraulic structures have been constructed in the VMD to protect agricultural crops, such as dyke rings, sluice gates, and culverts. These modifications have considerably changed the hydrodynamics in the VMD (Thanh et al., 2020a; Tran et al., 2018).

Tidal movement is the most important hydrodynamic forcing in estuarine areas. The Mekong Delta shows a complex interaction between semidiurnal tide from the East Sea and diurnal tide from the West Sea. Tidal range of the East Sea could reach up to 3.8 m and tidal amplitudes reduce gradually in the south-westerly direction. Tidal amplitudes in the West Sea are smaller, fluctuating in range between 0.5 and 1 m (Unverricht et al., 2013).

2.2. Sediment loads

There are two types of sediment loads towards the Mekong Delta. Suspended sediment loads at Kratie occupy 97% of the total sediment load while the bedload is only 3% (Koehnken, 2012). Therefore, we focus on the suspended sediment load in this study. Milliman and Syvitski (1992); Walling (2008) estimate the annual sediment load of the Mekong River to be 160 Mt/y. Sediment loads at Kratie fluctuated between 23 and 134 Mt/y from 1982 to 2004 with an average load of approximately 87 Mt/y (Darby et al., 2016), including extremely wet years (e.g. 2000). Koehnken (2014) estimated the annually averaged sediment load at Kratie from 2009 to 2013 slightly lower at about 73

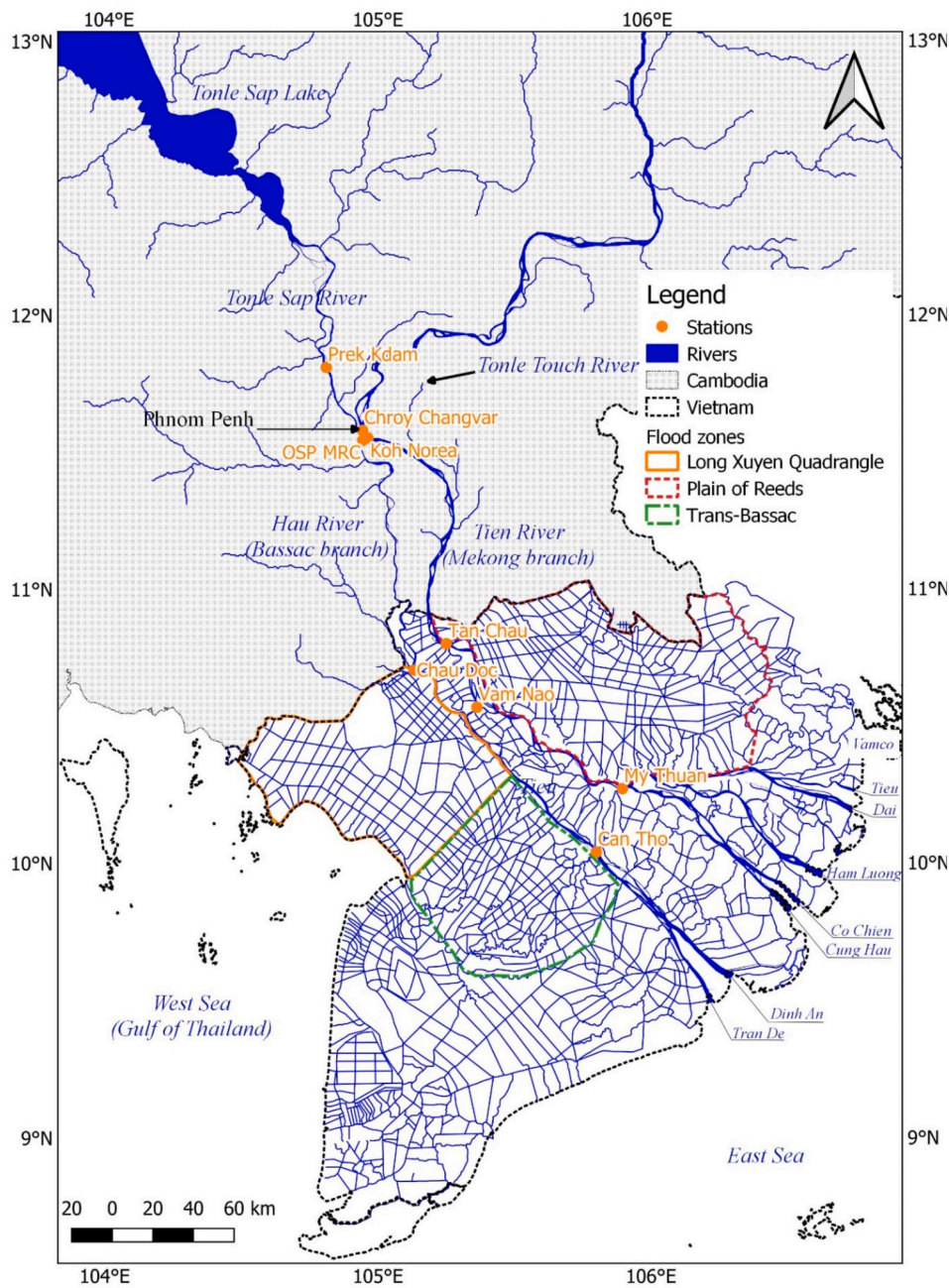


Fig. 1. Location of the mekong Delta.

Mt/y while the annual sediment load varied between 44 and 98 Mt/y in 2010 and 2011 respectively.

The Mekong River is subject to strong seasonal fluctuations and sediment loads vary accordingly. In general, sediment loads at Kratie in the high flow season (from July to October) provide approximately 95% of the annual sediment loads (Dang et al., 2018; Koehnken, 2014). The greatest sediment load usually occurs in September, supplying 25–40% of the annual load. In contrast, monthly sediment loads in the low flow seasons are extremely small, with a contribution of <1% of the annual load (Koehnken, 2014). From Kratie downstream, sediment loads are spatially correlated to local river flows in general, except for Tonle Sap River's sediment loads. Before the Mekong-Tonle Sap confluence, sediment loads at Chroy Chang Var (Fig. 1) are comparable to those at Kratie, with the highest suspended sediment load of about 1.4 Mt/day (Figure A1 in Appendix). At the Tonle Sap-Mekong confluence, most sediment is transported to the Mekong branch via Koh Norea station,

while the amount of sediment transported through the Bassac branch at station OSP MRC is much smaller, with a ratio of 1/6. The sediment flux into the Tonle Sap River mainly occurs during the early flood stage. The annual inflow into and outflow from the Tonle Sap River are about 6.4 Mt and 1.5 Mt (Koehnken, 2012). This ratio is consistent with model results computed by Kummur et al. (2008). The difference indicates the sediment trapping efficiency of Tonle Sap Lake, of around 80% (Sarkkula et al., 2010).

The Mekong (Song Tien) and Bassac (Song Hau) branches both supply suspended sediments to the VMD. The total sediment loads in 2011 were 50 Mt at Tan Chau on the Song Tien and 9 Mt at Chau Doc on the Song Hau (Manh et al., 2014). The connecting channel of Vam Nao diverted an amount of around 19 Mt from the Song Tien to the Song Hau in 2011 and balanced the sediment fluxes of the Song Tien and the Song Hau. As a result, sediment fluxes at My Thuan on the Song Tien and Can Tho on the Song Hau were approximately 26 and 29 Mt/y in 2011

(Manh et al., 2014). Nowacki et al. (2015) estimated that the Song Hau and the Song Tien mouths exported sediment amounts of 15 and 25 Mt/y in 2012–2013, respectively.

2.3. Suspended-sediment concentration

The suspended sediment concentration (SSC) in the Mekong Delta is typically smaller than 0.5 g/l (Koehnken, 2012; Manh et al., 2014), and is strongly modulated by the annual floods. In the Cambodian Mekong Delta, SSC in the Mekong River main tributaries fluctuates between 0.2 and 0.4 g/l during high flow seasons. The SSC on the Tonle Sap River is smaller than that on the Mekong River, with concentrations below 0.2 g/l (Koehnken, 2012). In the VMD, the hydrodynamics are not only influenced by the annual floods, but also by tides. At Can Tho station, the monthly average SSC is about 0.05 g/l, and it can increase to 0.18 g/l in the high flow seasons and decrease to 0.03 g/l in the low flow seasons. The SSC at ebb tides is slightly higher than at flood tides in the low flow seasons (Dang et al., 2018). This discrepancy increases in the high flow seasons (Dang et al., 2018). A similar pattern is found at My Thuan station, with slightly higher SSC. SSC near the Dinh An mouth was low, smaller than 0.03 g/l, in the high flow season (Nowacki et al., 2015).

2.4. Sediment grain size distribution

In general, suspended sediment grain sizes vary seasonally and spatially in the Mekong Delta. Grain-sizes of suspended sediment spatially decrease with distance downstream. Koehnken (2014) reported on a large-scale sediment monitoring campaign in the lower Mekong River. They found predominant cohesive sediments at Kratie. A small amount of fine sand was detected during high flow seasons. The suspended sediment load at Kratie comprises 20% of sand, 61% of silt, and 19% of clay materials. Finer sediments were found at Tan Chau, with proportions of 1%, 44%, and 54% for sand, silt, and clay respectively (Koehnken, 2014). Sarkkula et al. (2010) found that d_{50} is only 3–8 μm at Tonle Sap River and even finer in the Tonle Sap Lake. Hung et al. (2014) carried out an in-situ measurement of sedimentation in the upper VMD. Their results show that d_{50} is from 10 to 15 μm on the Plain of Reeds (PoR)'s floodplains (Wolanski et al., 1996). measured that d_{50} is from 2.5 to 3.9 μm in the freshwater regions of the Song Hau estuarine branch. An important sediment process in the estuarine reaches is flocculation that leads to flocs much larger than the individual grain sizes. For example, Wolanski et al. (1996) found that d_{50} of a floc is around 40 μm at the Song Hau estuary. This is consistent with the results presented by McLachlan et al. (2017) who show that the typical recorded sediment grain size is about 40 μm in the Song Hau estuary. Moreover, this size of flocs is similar to the typical sediment grain size found in the PoR's floodplains (Hung et al., 2014).

3. Methodology

3.1. Software description and model setup

3.1.1. Description of Delft3D FM

Hydrodynamics and sediment transport are modeled by flow and sediment transport modules which are combined in the Delft3D FM (DFM) modeling suite developed by Deltares (2020a). The DFM is the successor of Delft3D4 which has been widely used for hydrodynamic modeling of seas, rivers, and floodplains. DFM's noticeable improvement is the use of unstructured grids and concurrent multi-dimensional modeling, encompassing 1D, 2D, and 3D domains. Achete et al. (2016), Martyr-Koller et al. (2017), and Thanh et al. (2020a) provide examples of successful 2D and 3D DFM model descriptions and validation in estuarine environments.

The flow module of DFM solves the two- and three-dimensional shallow-water equations, based on the finite volume numerical method (Kernkamp et al., 2011). The 2D depth-averaged equations

describe mass and momentum conservation, as presented (Deltares, 2020b):

$$\frac{\partial h}{\partial t} + \nabla \cdot (hu) = 0 \quad (1)$$

$$\frac{\partial hu}{\partial t} + \nabla \cdot (huu) = -gh\nabla\zeta + \nabla \cdot (\nu h(\nabla u + \nabla u^T)) + \frac{\tau}{\rho} \quad (2)$$

where $\nabla = \left(\frac{\partial}{\partial x}, \frac{\partial}{\partial y} \right)^T$, ζ is the water level, h the water depth, u the velocity vector, g the gravitational acceleration, ν the viscosity, ρ the water mass density and τ is the bottom friction.

3.1.2. Model set-up

DFM allows computation on both curvilinear and unstructured grids so it is suitable for regions with complex geometry (Achete et al., 2015). In addition, it has multi-dimensional computations, especially combinations of 1D and 2D grids. This feature is efficient for considering small canals. Therefore, in this study, DFM is selected for simulating floods and sediment dynamics in the Mekong Delta which comprises a dense river network and highly variable river widths, flood plains, and hydraulic structures.

The large-scale hydrodynamic model of the Mekong Delta used in this study was well calibrated for the large floods in 2000 and 2001 (Thanh et al., 2020a). Unfortunately, suspended sediment data for these years were not comprehensively collected. Thus, the recent large flood in 2011 was used to validate hydrodynamics and calibrate sediment transport.

Our model setup improved prior model schematizations (Thanh et al., 2017; Van et al., 2012). The Mekong Delta is modeled using a combination of 1D networks and 2D meshes in a single computational domain. Additionally, hydrodynamics and sediment transport are computed based on an online coupling in contrast to Achete et al. (2016) who applied DelWAQ postprocessing on hydrodynamic model output to calculate sediment dynamics. Compared to the model used by Thanh et al. (2020a), the present model adds sluice gates to control water flow to selected regions. These sluice gates are located along the western part of the Mekong Delta and in the Quan Lo Phung Hiep region and prevent salinity intrusion into these regions (Hoanh et al., 2009).

3.1.2.1. Grid and bathymetry. Thanh et al. (2020a) describe in detail the computational grid and bathymetry presented in Fig. 3. The grid covers the lower Mekong River from Kratie, Cambodia, to its mouths and extends to about 80 km seawards of the coastline. The dense river network of the VMD is fully represented. The floodplains in the Mekong Delta incorporated in the model are based on the flood inundation maps (Dartmouth Flood Observatory, 2004).

The computational domain consists of a multi-dimensional grid that includes 1D and 2D connections. In the Mekong Delta, primary and secondary canals are represented in 1D networks while 2D cells are used for the Mekong River main channels, the floodplains, and the continental shelf. The 1D network has a uniform segment length of 0.4 km while the 2D cells have a different resolution depending on the spatial scale of the locally dominant morpho- and hydrodynamic processes. Specifically, the 2D cell sizes for the Mekong River mainstreams are approximately 0.7 km in general and decrease to about 0.2 km at river bifurcations and confluences. The 2D cells are coarser for floodplains and sea areas, increasing up to around 2 km in size. The grid totally contains 73,504 cells.

Detailed bathymetries of the Mekong Delta are sparse and limited. Therefore, the bathymetry is composed based on different sources (Fig. 2). The bathymetry of the Mekong Delta was extracted from the 1D-ISIS model that was used by the Mekong River Commission. Originally, the cross-sectional data was collected in 1998 and partly updated in 2015. The bathymetry of the Mekong River main channels was

interpolated from cross-sectional data of the 1D-ISIS hydrodynamic model for the Mekong Delta (Thanh et al., 2020b; Van et al., 2012). The bathymetry of the river mouths was updated by measured data in 2016. The 1D network of primary and secondary canals are defined by cross-sections originally extracted from the 1D-ISIS model. For the sea areas, it is imposed from ETOPO of about 1 km resolution. The floodplain topography is obtained from the digital elevation model, with a resolution of 250 m provided by the Mekong River Commission. The estuarine branches were updated by recent in-situ data (Thanh et al., 2017).

3.1.2.2. Sediment transport equation. Suspended sediment occupies the majority proportion of total sediment load in the Mekong Delta and sediment bedload is about 3% of suspended sediment load (Koehnken, 2014). Therefore, this research only considers suspended sediment load for modeling. Hung et al. (2014) found that medium grain sizes of suspended sediment in floodplains fluctuate in ranges of 10 and 15 μm . In the Mekong Delta, Koehnken, 2014 found a predominance of silt and clay at Kratie and Tan Chau stations, respectively. Consequently, cohesive sediment is the only sediment fraction used in this study (Thanh et al., 2017). We neglect vertical stratification, but the effect of flocculation due to salinity is included, by applying a larger fall velocity in saline water.

Suspended sediment transport is computed by online coupling between the flow and sediment transport modules of the DFM suite. Sediment transport is formulated by the 2D advection-diffusion equation for suspended sediment (Deltares, 2020a).

$$\frac{\partial c^{(l)}}{\partial t} + \frac{\partial uc^{(l)}}{\partial x} + \frac{\partial vc^{(l)}}{\partial y} - \frac{\partial}{\partial x} \left(D_x \frac{\partial c^{(l)}}{\partial x} \right) - \frac{\partial}{\partial y} \left(D_y \frac{\partial c^{(l)}}{\partial y} \right) = 0 \quad (3)$$

where $c^{(l)}$ is mass concentration of sediment fraction (l) (g/l); u and v are flow velocity components (m/s); D_x and D_y are the diffusion coefficients in x and y directions respectively (m^2/s).

Erosion and sedimentation in a cell are described by the well-known Krone-Partheniades equations (Partheniades, 1965):

$$E = M \left(\frac{\tau_b}{\tau_e} - 1 \right) \quad (4)$$

$$D = w_s c \left(1 - \frac{\tau_b}{\tau_d} \right) \quad (5)$$

where E is the erosion flux ($\text{kg/m}^2/\text{s}$), M is the erosion parameter ($\text{kg/m}^2/\text{s}$), τ_b is the bed shear stress (N/m^2), τ_e is the critical shear stress for erosion, D is the deposition flux ($\text{kg/m}^2/\text{s}$), w_s is the settling velocity (m/s), c is near-bed suspended sediment concentration (kg/m^3) and τ_d is the critical shear stress for deposition (N/m^2). Equation (5) is approximated as ($D = w_s c$) when τ_d is much larger than τ_b (Achete et al., 2015; Deltares, 2020a; Winterwerp et al., 2006).

3.1.2.3. Boundary conditions. For hydrodynamic forcing, we defined water discharges at Kratie (the upper boundary) and water levels at the ocean (the lower boundary). In addition, the lateral offshore boundary is specified as a Neumann boundary which allows free development of cross-shore water level slopes (Roelvink and Walstra, 2004). The water discharges at Kratie are generated by measured water levels and the updated rating curve created by the Mekong River Commission (MRC). The measured water levels are collected from the near real-time hydro-meteorological monitoring system of MRC (<https://monitoring.mrcmekong.org/station/014901>). The water levels at the ocean are imposed by the eight main astronomical tidal constituents derived from the global tidal model of TPXO 8.2 (Egbert and Erofeeva, 2002). Local precipitation is neglected because this study focuses on river flows.

For the lower boundary, SSC is set to 0 g/l because the river plumes are well contained within the computational grid (Thanh et al., 2017) in

contrast to Manh et al. (2014) who defined the downstream boundary conditions at the Mekong River mouths from water turbidity derived from satellite images. These data have a temporal interval of around a week. However, measured data of suspended-sediment concentration at the Mekong River mouths are highly variable based on a tidal fluctuation. For example (Nowacki et al., 2015), found that SSC on ebbs is considerably greater than on floods, suggesting that the boundary condition of SSC at these mouths needs a higher temporal resolution. Unfortunately, measurements at these stations with the required temporal frequency are not available. Therefore, the model grid was extended to completely contain the sediment plumes.

The upper boundary SSC at Kratie is not measured frequently. Therefore, we derived SSC from a regression curve with water discharges. This method is commonly used to generate SSC data in the Mekong River (Darby et al., 2016; Koehnken, 2012; Kummur and Varis, 2007; Lu et al., 2014; Lu and Siew, 2006; Manh et al., 2014; Walling, 2008).

Table 1 shows empirically derived relationships between measured SSC and discharge for Kratie by Darby et al. (2016), Koehnken (2012), and Manh et al. (2014). Applied to measured flow at Kratie, Fig. 3 shows the derived 2011 sediment loads. Darby et al. (2016)'s curve predicts higher SSC since it is based on a much longer period of data analysis that includes the effect of sediment load decline due to upstream dam construction (Darby et al., 2016; Kummur and Varis, 2007; Lu and Siew, 2006). Consequently, SSC generated by Koehnken (2012) is more reliable for recent years and is used as boundary conditions because we estimate a sediment budget for the VMD in recent years. Thus, the Darby et al. (2016)'s curve was not used since it happens in the pre-dam periods.

3.1.2.4. Wave modeling. Our modeling domain includes the shelf of the Mekong Delta where waves strongly influence hydrodynamics and sedimentation processes (Thanh et al., 2017). The waves at the shelf of the Mekong Delta are generated by monsoon winds (northeastern and southwestern monsoons).

Waves are computed by the Delft3D-Wave, which is a third-generation SWAN model. Tu et al. (2019) calibrated this model against measured data for this region. The wave model couples with the flow model at 1-h intervals. The wave data which were derived from ERA Interim reanalysis data (<https://apps.ecmwf.int/datasets/data/interim-full-daily>), were imposed at the offshore boundary. The boundary conditions consist of wave height, wave period, and wave direction. The wave heights off the west and east coasts of the Mekong Delta are significantly different (ADB, 2013), necessitating spatial variation in the imposed boundary conditions.

3.1.2.5. Initial conditions. Hydrodynamics in the Mekong Delta are strongly driven by the annual floods. Moreover, the Tonle Sap Lake plays a crucial role in regulating river flows the delta downstream. Water levels of the Tonle Sap Lake vary seasonally to a large extent. Therefore, correct specification of initial conditions reduces model spin-up periods.

Table 1

SSC rating curves for Kratie station, with SSC is suspended-sediment concentration and Q is flow discharge at Kratie station ($\text{m}^3 \text{s}^{-1}$).

Studies	SSC (mg/l)	Estimated annual sediment load in 2011 (Mt)	Analysis period
Koehnken (2012)	$0.13332 * Q^{0.7098}$	98	2011
Manh et al. (2014)	$10^{(-494.02 * \log(Q) - 4.52 + 2.88)}$	96	2010–2011
Darby et al. (2016)	$0.3002 * Q^{0.8967}$	156	1981–2005

We assume that a previous flood filled the Tonle Sap Lake. Therefore, the model was spun up over the flood of 2010 and we used water levels at the end of 2010 as the initial conditions for the year 2011 simulations. Over the model domain, a uniform value of 0 g/l was set as initial conditions of SSC, since SSC is low in the low flow seasons. We used model settings for hydrodynamic parameters following Thanh et al. (2020a, 2017) including the calibrated values of the Manning roughness coefficient spatially varying in the range of 0.016–0.032. The initial bed sediment layer thickness was uniformly set at 10 m, which allows abundant sediment availability for the simulated period.

3.2. Sediment properties

For modeling cohesive sediment dynamics, we need to specify, critical bed shear stress for erosion (τ_{ce}), erosion rate (M), and settling velocity of sediment (w). McLachlan et al. (2017) measured shear stresses in-situ at the Song Hau estuarine branch and estimated the highest shear stress at approximately 10 Pa. However, Vinh et al. (2016) set τ_{ce} of 0.2 N/m² for the coastal VMD while the amplitude of τ_{ce} on the VMD floodplains fluctuated in the range of 0.028–0.044 N/m² (Hung et al., 2014). M was in the range of 5.1×10^{-6} - 8.8×10^{-5} kg/m²/s and a reasonable value for modeling is 2×10^{-5} kg/m²/s (Hung et al., 2014; Thanh et al., 2017; Vinh et al., 2016).

The settling velocity in the Mekong River is highly variable depending on the local hydrodynamics and salinity. Manh et al. (2014) mention that the calibrated w value in the main channels of the Mekong River was 1.3×10^{-3} m/s. Hung et al. (2014) calculated that settling velocities on the VMD floodplains fluctuated from 2.2×10^{-4} to 1.8×10^{-3} m/s. McLachlan et al. (2017) estimated settling velocities on the Song Hau estuarine branch to be much smaller, with an average magnitude of around 5×10^{-5} m/s. Furthermore, w is also influenced in saline waters by growing flocs. For instance, Wolanski et al. (1996) observed that the median size of flocs in the Mekong estuary ranges between 50 and 200 μ m and this changes the sediment settling velocity. Vinh et al. (2016) revealed that w in fresh and saline waters were 5×10^{-5} and 3.25×10^{-4} m/s, respectively.

3.3. Calibration

Percent bias (PBIAS) and index of agreement (Skill) are commonly used statistical indices to evaluate model performance (Achete et al., 2015; Ferré et al., 2010; Ji, 2017; Thanh et al., 2017; Van Liew et al., 2007). These indices are calculated as

$$PBIAS = \frac{\overline{S-M}}{\overline{M}} \quad (6)$$

$$Skill = 1 - \frac{\sum (S-M)^2}{\sum (|M-\overline{O}| + |O-\overline{O}|)^2} \quad (7)$$

where S and M are simulated and measured SSC, respectively; and \overline{M} and \overline{O} are time average measured SSC.

PBIAS and Skill were used to assess simulated discharge and SSC at mainstream stations. PBIAS values present the average tendency of simulated results. A perfect PBIAS value of 0 illustrates that modeled results are completely unbiased. Positive and negative PBIAS values indicate model biases toward overestimation and underestimation, respectively. Skill was introduced by Willmott (1981) and it presents how accurate the model estimates the variation in measured data. Skill values range from 0 to 1 in which the value of 1 indicates that simulations and observations have perfect agreement while the value of 0 shows disagreement between them. A well calibrated model should have values of $|PBIAS| < 0.25$ and Skill > 0.2 (Ji, 2017; Moriasi et al., 2007). Table 2 depicts categories of model performance intervals.

Table 2

Qualification of model performance indicated by PBIAS and Skill indexes.

Qualification	$ PBIAS $	Skill
Excellent	< 0.1	1.0 – 0.65
Good	0.1 – 0.15	0.65 – 0.5
Reasonable/fair	0.15 – 0.25	0.5 – 0.2
Poor	> 0.25	< 0.2

4. Results and discussion

4.1. Model calibration and validation

4.1.1. Hydrodynamic and salinity calibration

Detailed results of model performance for water discharge at stations on the mainstream of the Mekong River are illustrated in Table 3. These stations are selected to validate the model since the data are available for the chosen year. However, these stations can represent flood propagation along the Mekong River as they are located from the upstream boundary (Kratie) to the strongly tide-dominated areas (Can Tho and My Thuan). The model reasonably simulates water discharge in the delta because the values of statistical indexes at these stations are higher than the reasonable value, except Chau Doc station. Skill values of these stations are higher than 0.8 which classifies them as excellent. Generally, the model slightly underestimates water discharge as PBIAS values are negative.

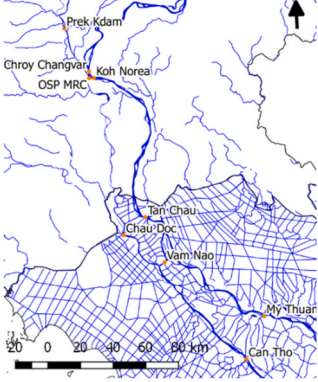
The fall velocity of cohesive sediment is influenced by salinity, which enhances flocculation processes (Mhahshah et al., 2018; Portela et al., 2013). In the Mekong Delta, Wolanski et al., 1996 found that sizes of flocs in the saltwater region are much larger than those of suspended sediment grains. The length of saltwater intrusion into the Mekong River is approximately 50 km from the river mouth (Nguyen and Savenije, 2006; Nowacki et al., 2015; Wolanski et al., 1998). Salinity intrusion into the Song Hau is limited by seasonally varying river flow (see An Lac Tay station in Fig. 4). The largest salinity intrusion occurs during the low flow season, while the water at the river mouths is nearly fresh in the high flow seasons (Wolanski et al., 1996). As a result, the salinity is only measured in the low flow seasons, so the calibration period of salinity did not include the period Jul–Dec 2011.

Fig. 4 shows that simulated and measured salinity is in reasonable agreement. The 2D model is capable of modeling the seasonal and tidal cycle variations of salinity. Specifically, the highest salinity at Tran De station is about 20 ppt during the low flow season. We calibrated salinity intrusion by adapting the horizontal eddy diffusion coefficient leading to a value of $450 \text{ m}^2 \text{ s}^{-1}$ constants over the model domain. This high value was also found in other modeling studies and is caused by considerable sub-grid-scale processes (Talley et al., 2011).

4.1.2. Sediment dynamics calibration

To calibrate the sediment dynamics model, we adapted and modified the proposed approach of alternative settings developed by Van Maren and Cronin (2016). Specifically, the settling velocity and the critical shear stresses were estimated based on available measured data. The settling velocities in fresh water and saltwater are well measured and applied in numerical modeling (Le et al., 2018; Thanh et al., 2017; Vinh

Table 3
Statistical indexes of model performance of water discharge, suspended-sediment concentration, and sediment flux.



Station	Discharge		SSC		Daily Sediment Flux	
	PBIAS (%)	Skill	PBIAS (%)	Skill	PBIAS (%)	Skill
Chroy Changvar	-6	0.98	25	0.63	11	0.83
Koh Norea	-16	0.86	N/A	N/A	-7	0.86
OSP MRC	N/A	N/A	5	0.72	-8	0.91
Prek Kdam	N/A	N/A	N/A	N/A	-40	0.56
Tan Chau	-4	0.99	61	0.90	36	0.93
Chau Doc	-33	0.85	-18	0.78	-45	0.67
Vam Nao	N/A	N/A	N/A	0.90	N/A	N/A
My Thuan	-18	0.94	16	0.94	-23	0.86
Can Tho	-12	0.97	7	0.87	-20	0.73

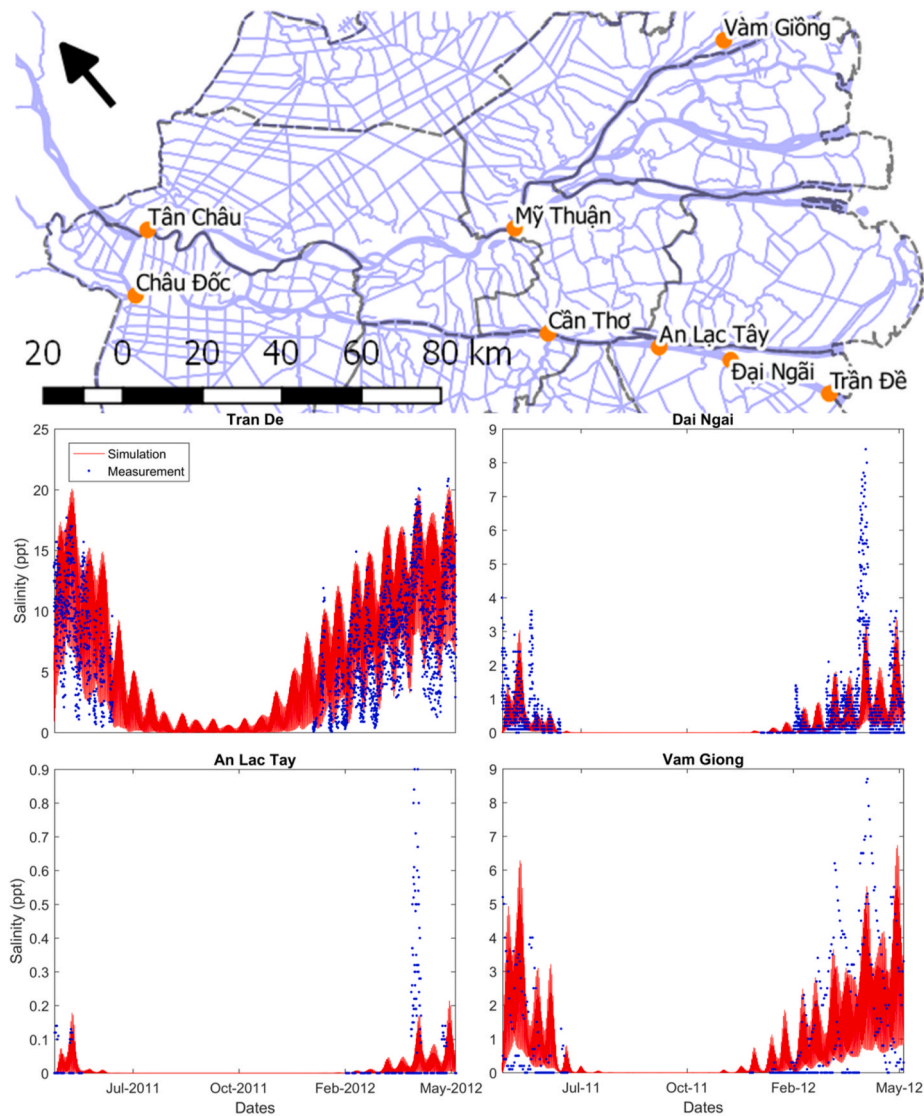


Fig. 4. Measured (in blue) and simulated (in red) salinity at Tran De, Dai Ngai, An Lac Tay, and Vam Gieng.

et al., 2016). We calibrated to lower the sediment flux by increasing the critical shear stress and decreasing the erosion rate.

The model was calibrated against measured SSC data in the high-flow 2011 season and the low-flow 2012 season focusing on stations along the Mekong River. The order of the low-flow and high-flow seasons is of great importance. This order not only plays a considerable role in controlling seasonal variations of the Mekong River flow but also in sediment trapping. We select the low-flow season after the high-flow season because of the regulation of the Tonle Sap Lake.

The parameters of roughness, τ_{ce} , M , and w have considerable impacts on sediment dynamics (Achete et al., 2015; Manh et al., 2014). Roughness coefficients are not an efficient calibrated parameter for the sediment model because they are evaluated in hydrodynamic calibration and this eliminates a free variable in sediment calibration (Gibson et al., 2017). The settling velocity was not considered as a calibration parameter, because it is well measured and successfully used in other numerical studies (Gratiot et al., 2017; Le et al., 2018; Marchesiello et al., 2019; McLachlan et al., 2017; Thanh et al., 2017; Tu et al., 2019; Vinh et al., 2016). The w was set to 5×10^{-5} m/s and 3.5×10^{-4} m/s for fresh and saline waters, respectively, with interpolated values for brackish environments. Recent measurements by Gratiot et al. (2017) and Le et al. (2018) have a reasonable agreement with these settling velocities.

The calibration ranges of τ_{ce} and M were chosen from measurements of prior studies (e.g. Berlamonta et al., 1993; Hung et al., 2014a; Manh et al., 2014; McLachlan et al., 2017; Vinh et al., 2016). The selected ranges for the two parameters were for τ_{ce} 0.3–0.5 N/m² and for M 10^{-5} – 10^{-6} kg/m²/s.

In general, calibration simulations overestimate SSC on the Mekong River (Fig. 5). The model clearly produces seasonal variations of SSC that are strongly dominated by the annual floods, which is reflected by high skill values (Table 3). In addition, SSC also varies with spring-neap cycles at Can Tho and My Thuan stations where tidal influence is high. Within the selected calibration range, M has a much stronger influence on SSC than τ_{ce} and this can be explained by the bed erosion flux computed by Equation (4). The curves and peaks timing of simulated

SSC resemble observed SSC. It is noted that the smallest τ_{ce} and the highest M in the selected ranges result in unrealistic SSC (>1 g/l). SSC at Chau Doc is underestimated probably due to the underestimation of water discharge at Chau Doc station (Table 3).

The measured sediment fluxes are estimated from daily average discharge and SSC at stations on the mainstream Mekong River (Fig. 5 and Figure A5 in Appendix) and compare well with modeled behavior. The model parameter set which results in the best fit of simulated and measured suspended-sediment concentration and sediment transport has a τ_{ce} value of 0.3 N/m² and a value for M of 10^{-6} kg/m²/s.

During the calibration process of SSC, we found that the varying dominant hydrodynamic factors across the model domain, strongly influence the results of model calibration. For example, the run which has τ_{ce} of 0.6 N/m² and M of 8×10^{-5} kg/m²/s, compares well with measured data at the fluvial-dominant stations while it highly underestimates SSC at the tide-dominant stations. The initial SSC and bed sediment availability had a very limited impact on the calibration. This is in contrast with Achete et al. (2015) who found that initializing the model with bed sediment could cause a high SSC and take around 5 years to be reworked and with van Kessel et al. (2011) who revealed that a simulation with no bed sediment could take up to 3 years in order to reach the equilibrium conditions. For our study, Fig. 5 shows that the simulation period begins in the low flow season (from May 2011) at which the SSC is low, so the model takes a short spin-up time of around two weeks. Bed-sediment availability is essential to skillfully model SSC in the Mekong Delta. For example, at some stations (e.g. Chroy Changvar and OSP MRC) SSC is slightly higher than those at Kratie (the only source of sediment in modeling). Probably the abundance of sediment available in the Mekong River bed makes model calibration less subject to bed sediment definitions and initial SSC as reported by Achete et al. (2015) and van Kessel et al. (2011).

4.2. Hysteresis relations of suspended-sediment concentration and water discharge

Our model is able to reproduce SSC hysteresis during a river flood

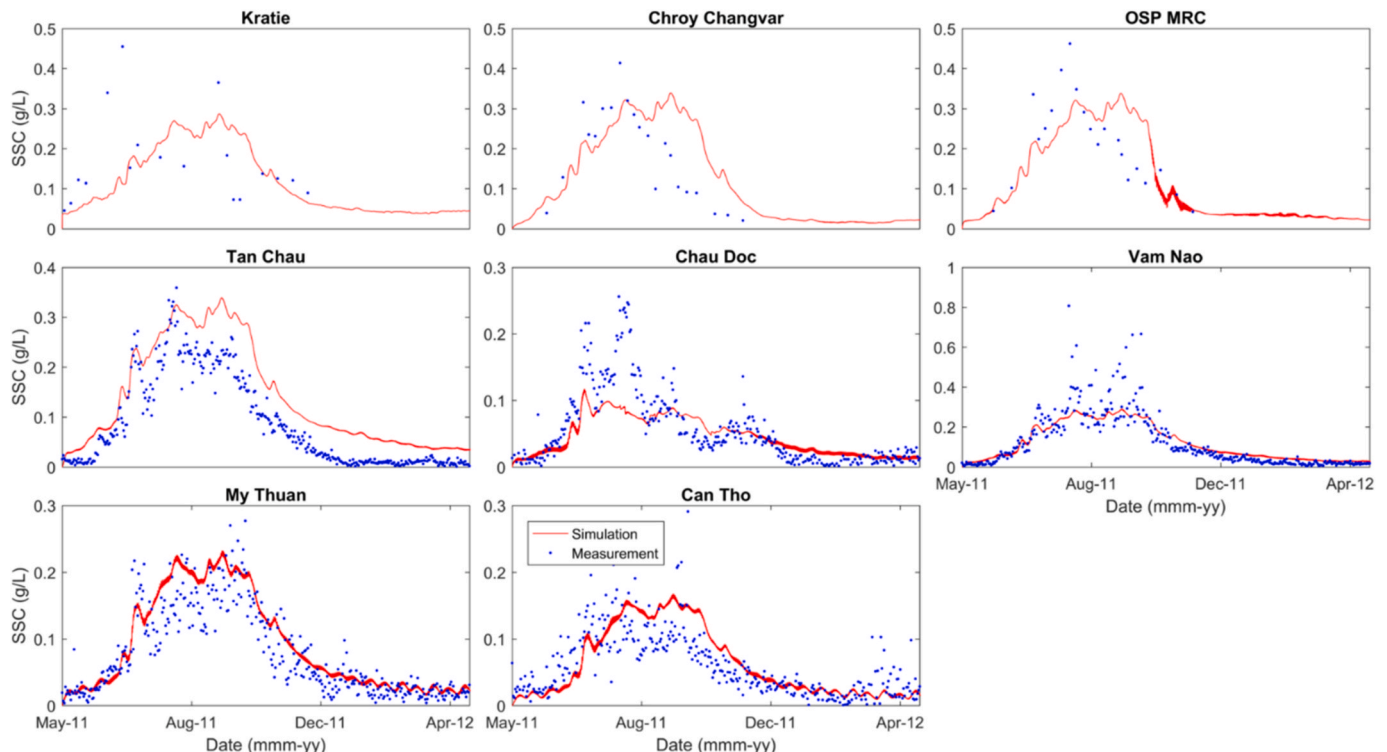


Fig. 5. Comparison of modeled and measured suspended-sediment concentration.

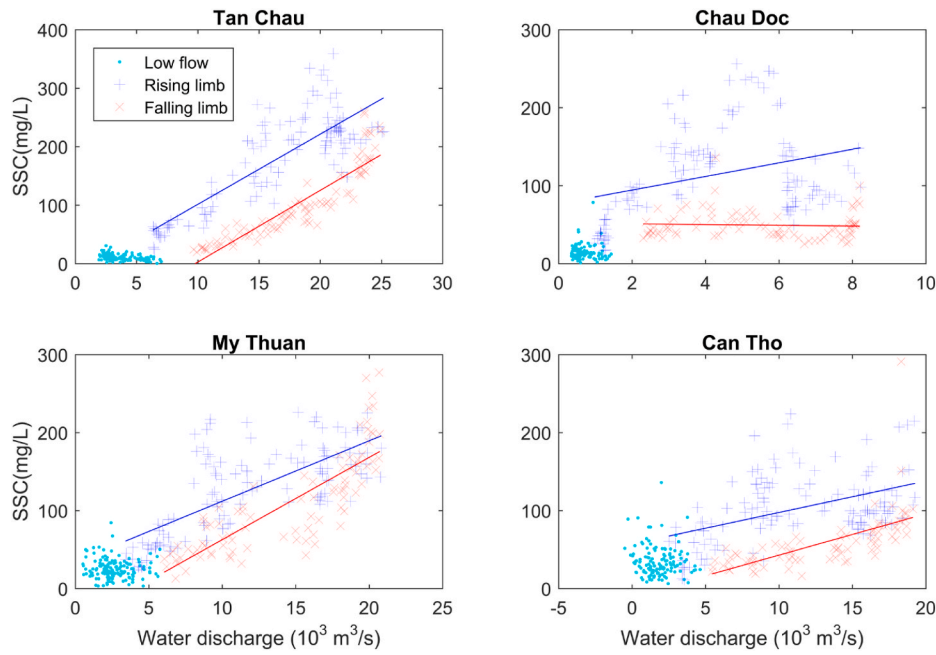


Fig. 6. Relationship between daily averaged measured suspended-sediment concentration and water daily averaged discharge at four stations, namely Tan Chau, Chau Doc, My Thuan, and Can Tho. Low flow conditions are from January to June 2011. The rising phase begins from June to the yearly discharge peak in September, whereas the falling phase is taken from September to January 2011.

(Fig. 6) with SSC being higher during the rising phase of the river flood than during the falling tide of the river flood. Fig. 6 clearly indicates the characteristic clockwise loops at different stations (Williams, 1989), with the SSC peak occurring earlier than the discharge peak. A general mechanism for SSC hysteresis is an early suspension of easily erodible sediments at the start of the river flood (Landers and Sturm, 2013). Walling (2008) observed the SSC hysteresis which reflects sediment remobilization of the Mekong River. However, our modeling effort did not define that process since we applied a single sediment fraction with constant properties throughout the model runs. Also, the SSC hysteresis does not stem from the boundary since SSC at the boundary was defined by a direct relationship between river flow and SSC at Kratie.

Instead, we found that the main factor causing modeled SSC hysteresis is the sediment trapping of the Tonle Sap Lake. The sediment trapping decreases the SSC of outflows significantly compared to inflows. During a rising river flood, flood flow with high SSC from the Mekong River diverts to the Tonle Sap River at Prek Kdam to fill the Lake (Fig. 7a). The sediment largely deposits in the lake. For example, Kummur et al. (2008) found that around 80% of sediment which is stored in the lake and its floodplains, is from the Mekong River and tributaries. In the late high-flow season, the flow of the Tonle Sap River reverses when water levels on the Tonle Sap Lake are higher than those on the Mekong River (Fujii et al., 2003; Kummur et al., 2014; Thanh et al., 2020a). Although SSC on the Mekong River is still high (~200 mg/l), the

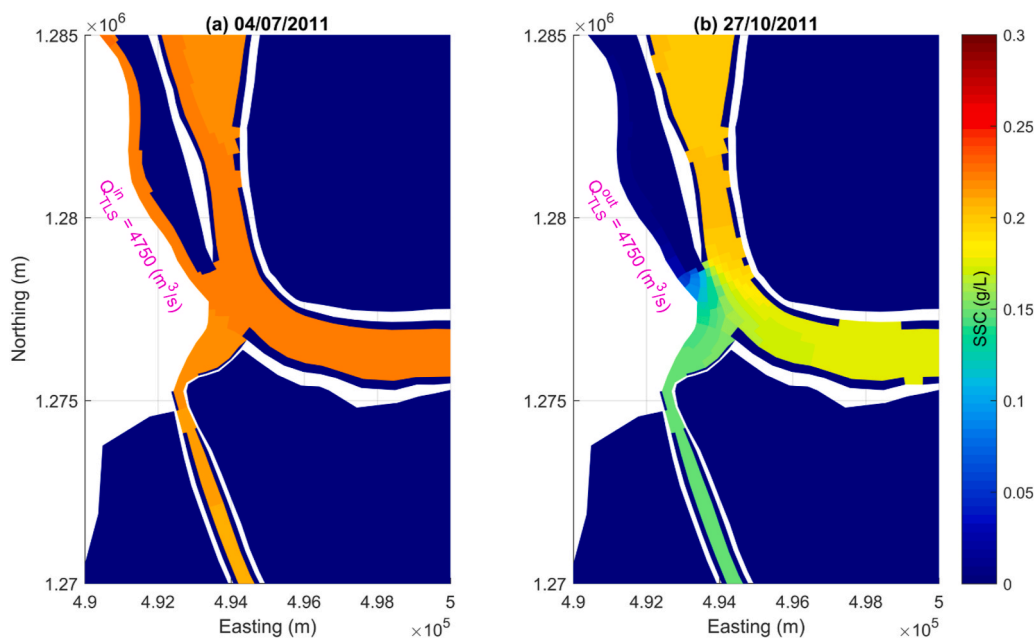


Fig. 7. Spatial variation of modeled suspended-sediment concentration during inflows (a) and outflows (b) of the Tonle Sap River.

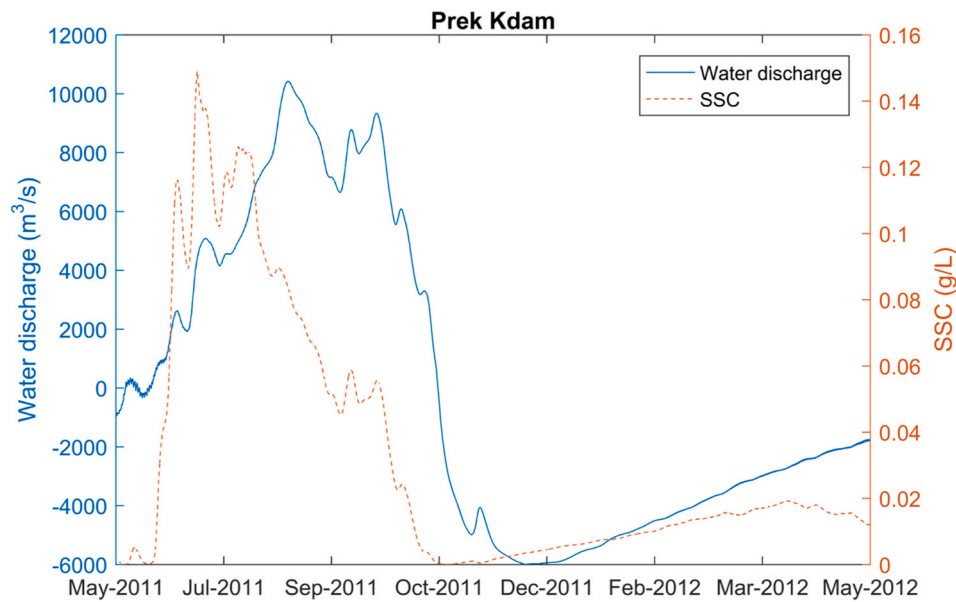


Fig. 8. Temporal variation of modeled water discharge and suspended-sediment concentration at Prek Kdam (Tonle Sap River).

low SSC water from the Tonle Sap River (~20 mg/l) mixes with the Mekong River flow at the Phnom Penh confluence reducing SSC in the confluence downstream (Fig. 7b). Our model adequately captures these sediment dynamics (Fig. 8). Our finding confirms estimates by Kummur et al. (2008)'s of an annual sediment deposition of about 5.7 Mt in the Tonle Sap Lake.

It should be noted that our model did not consider tributaries of the Tonle Sap catchment. The tributaries contribute up to about 30% of the inflow into the Tonle Sap Lake (Kummur et al., 2008) and supply a sediment amount of about 2 Mt/y (Kummur et al., 2008; Lu et al., 2014). With additional flows from Tonle Sap tributaries, outflows from the Tonle Sap Lake would increase slightly, with slightly higher SSC, increasing sediment fluxes from the Tonle Sap River to the Mekong River. The connection to the Tonle Sap Lake plays a critical role in regulating flows in the Mekong Delta and the Tonle Sap Lake received about 3.7 Mt in 2011 which resulted from differences between inflows and outflows of the Tonle Sap Lake. The discrepancies between inflows and outflows of the Tonle Sap Lake are still under discussion. Recent

studies show opposite results on sediment transport of the Tonle Sap Lake (Kummur et al., 2008; Lu et al., 2014). They used measured discharge and SSC to investigate whether the Tonle Sap Lake receives sediment from or supplies sediment to the Mekong River. Interestingly, Kummur et al. (2008) found that the lake receives a net sediment amount of about 5.7 Mt/y, in which sediments are transported from the Mekong River and Tonle Sap tributaries around 7 Mt/y and supply about 1.38 Mt/y to the Mekong River in the outflow period. In contrast, Lu et al. (2014) estimated that the mean sediment inflow and outflow are 6.3 Mt and 7 Mt, respectively. This means the Tonle Sap Lake supplies about 0.7 Mt. This estimate may be incorrect due to a limitation of data used and this study is opposite to some estimates (Koehnken, 2012, 2014; Kummur et al., 2008; Manh et al., 2014).

4.3. Seasonal variation of suspended sediment

This section describes spatial and temporal variations of modeled SSC in the Mekong Delta which consists of different hydrodynamic

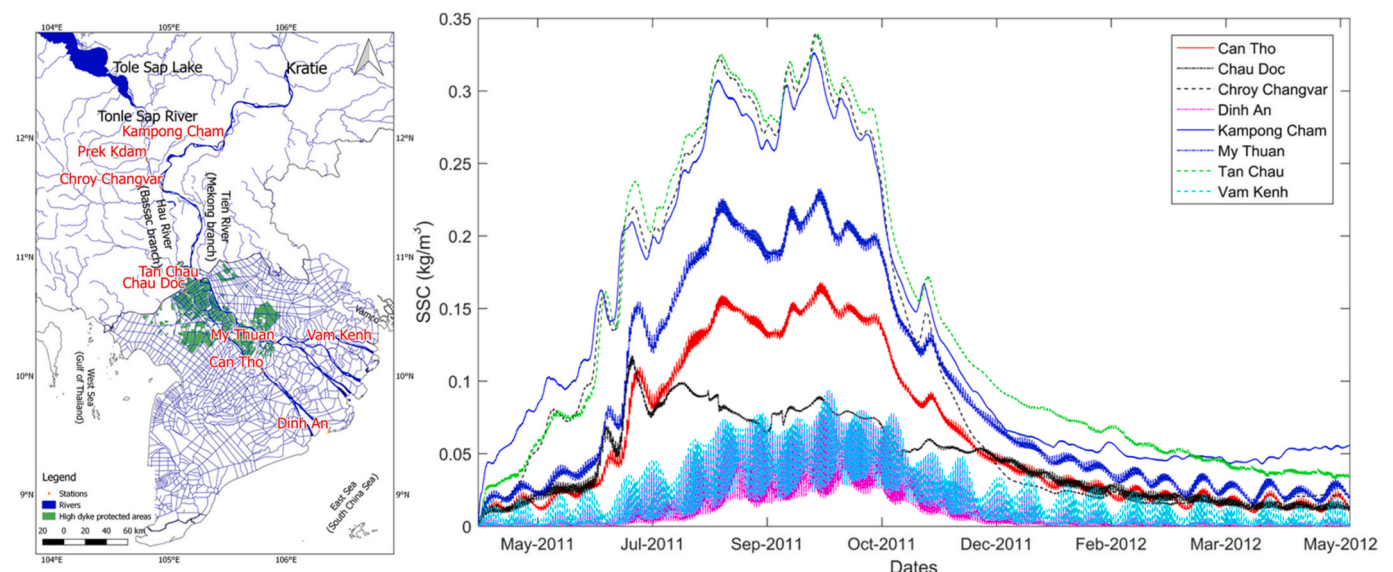


Fig. 9. Separated regions in the Mekong Delta based on hydrodynamic conditions and SSC variation in these regions.

regions. Fig. 9 shows hourly simulated SSC at some selected stations in the Mekong River. In general, SSC at these stations varies significantly throughout the selected period. The SSC is highest in August and September, and lowest in March. These variations are strongly dominated by the annual floods, so they have similar seasonal variability, but the magnitudes are different between these stations. The differences result from the sediment availability in the channel system. For instance, the SSC peaks at Kampong Cham (upper station) are slightly lower than those at Chroy Changvar and Tan Chau (lower stations). This implies that there is an additional source of sediment which affects SSC in the Mekong River. The reason is that sediment modeling included sediment availability in the channel system. This is in line with the presence of bed-sediment availability within the Mekong channel system, CMD, as observed by Walling (2008).

In the CMD, SSCs at Kampong Cham increase rapidly coinciding with flows in the high flow season. The highest value is about 0.35 g/l in the high flow season while SSCs fluctuate around 0.05 g/l in the low flow season. The river flow is the dominant hydrodynamic factor in this region, so SSCs fluctuate with the river flow. Besides, the floodplains in

this region also have an insignificant impact on SSC. Downstream of the Tonle Sap-Mekong confluence, SSCs are considerably influenced by the interaction of the Tonle Sap River and Mekong River. On the Tonle Sap River, SSCs of the inflows (Mekong River to Tonle Sap Lake) are significantly higher than in the reversal flows, reflecting the sediment transport to and efficient trapping of the Tonle Sap Lake.

The VMD receives sediment from the Song Tien, the Song Hau, and Cambodian floodplains. At Tan Chau, SSC variations are high in the high flow season, comparable to SSCs at Chroy Changvar while they show tidal variations during the low flow season. In the VMD middle, the tides strongly drive sediment fluctuations in both the high flow and low flow seasons. In the high flow season, the highest SSC can reach 0.25 g/l at My Thuan and 0.2 g/l at Can Tho. In the low flow seasons, SSCs obviously vary with spring-neap cycles, fluctuating from 0.025 to 0.05 g/l. These values are completely consistent with the analysis by Dang et al. (2018). SSCs during ebb tides are marginally higher than those during flood tides. This asymmetry causes a seaward flux of suspended sediment. At the mouths of the Mekong River, SSCs fluctuate in the range of 0.01–0.1 g/l in the high flow season, coinciding with tidal variations

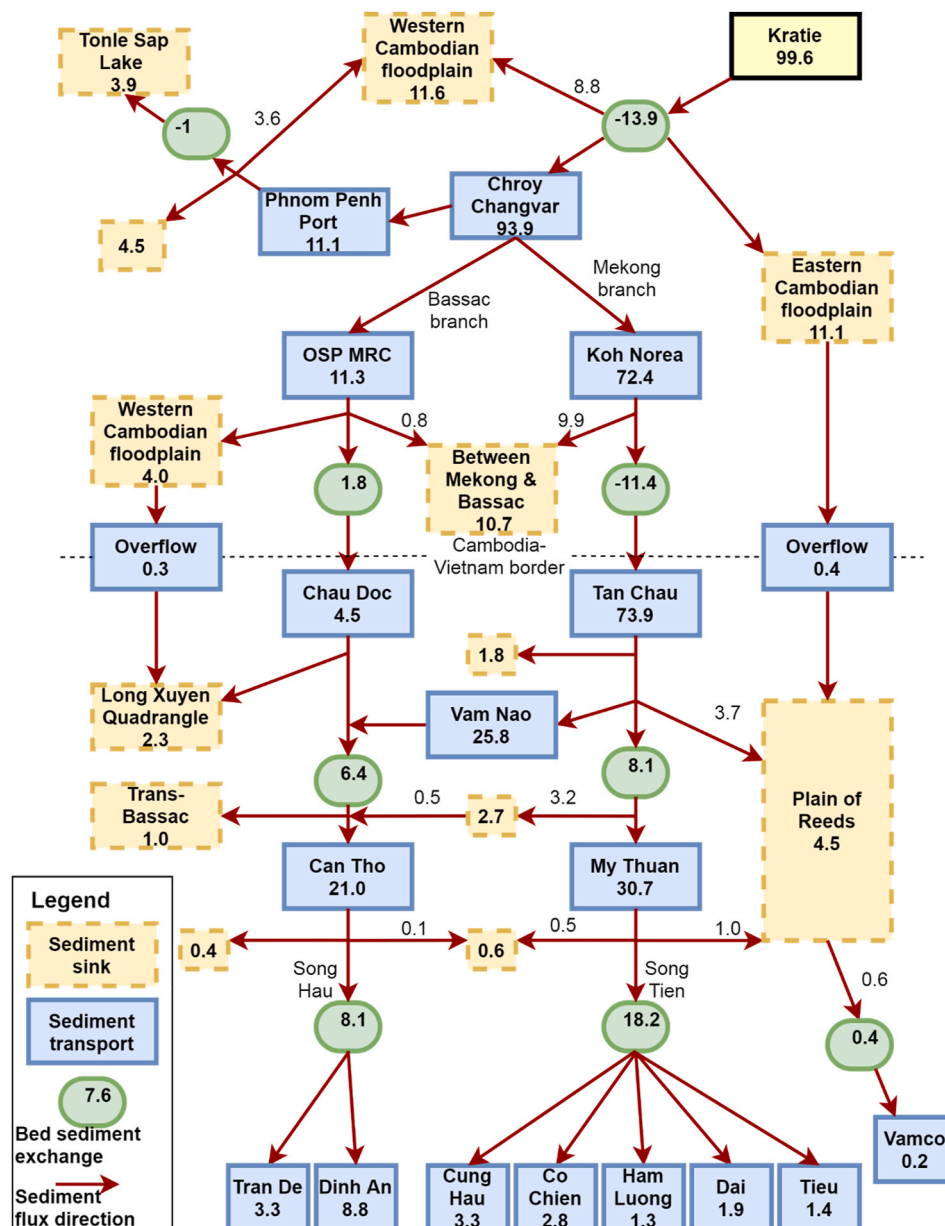


Fig. 10. Modeled sediment budget (in Mt) of the Mekong Delta, location names are indicated in Figs. 1 and 2.

while they are smaller than 0.05 g/l in the low flow season. These simulated values of SSC are slightly lower than measured data analyzed by McLachlan et al. (2017). There are several factors contributing to the differences such as salinity stratigraphy, estuarine turbidity maximum, and flocculation. The salinity stratigraphy was neglected since a 2D depth-averaged model setup was used while the flocculation was taken into modeling by changing settling velocities in freshwater and saltwater.

4.4. Sediment budget

The Mekong River at Kratie supplied more than 99 Mt of suspended sediment that was transported towards the Mekong Delta from June 2011 to June 2012. Based on our model validation at specific sites, we can now derive a sediment budget describing the distribution of these sediments within the Mekong Delta, illustrated in Fig. 10.

The river flood erodes the river channel of the Mekong from Kratie to Phnom Penh by around 13.9 Mt of sediment while the adjacent floodplains receive an amount of 8 Mt (northern floodplain) and 11.1 Mt (southern floodplain) during the high-flow season. Approximately 94 Mt flows into the Mekong Delta at Phnom Penh. At Phnom Penh, the Mekong River connects to the Tonle Sap River which transports 11.1 Mt. During rising river flood, the Tonle Sap River transports 4.5 Mt to the Lake, whereas the Tonle Sap River transports 0.6 Mt to the Mekong River during the falling river flood. The net result is a supply of 3.9 Mt to the Lake. Downstream of Phnom Penh the Mekong River separates into two branches, namely Mekong and Bassac (see Fig. 1), transporting 72.4 Mt (73 %) and 11.3 Mt (11 %) seaward, respectively. An additional amount of 0.7 Mt (0.7 %) is delivered over the floodplains between Vietnam and Cambodia. This portion is slightly higher than estimates (64–71%) of Manh et al. (2014). The difference is probably due to the inclusion of bed-sediment availability in this study.

The percentage of the total sediment supply at Kratie transported into the VMD by the main channels depends on water years. In wet years, the percentage is smaller than this in the dry years. The sediment trapping of the Cambodian floodplain and Tonle Sap system in the wet years is higher than that in the dry years (Manh et al., 2014).

Suspended sediments are transported into the VMD by the Mekong branch (Tien River), the Bassac branch (Hau River), and floodplain flows. Among these ways, the Tien River is the major way that conveys about 74 Mt at Tan Chau, accounting for 93% of the total sediment discharge towards the VMD. The overland flows transport small amounts of sediment during the high-flow seasons.

In the VMD, river flows and sediment transport are strongly affected by the dense man-made canal system so sediment transport in the VMD is complicated, especially the interaction between the Tien River, the Hau River, and the floodplains. The canals between the Tien River and the Hau River divert water and sediment from the Tien River to the Hau River due to the slightly higher water level in the Tien River. The water discharge in the Tien River and Hau River becomes similar from the connecting canal (Vam Nao) seaward (Dang et al., 2018; Thanh et al., 2020a). The Vam Nao canal diverts ~25.8 Mt from the Tien River to the Hau River. However, sediment fluxes at My Thuan (30.7 Mt) are slightly higher than at Can Tho (21.0 Mt).

The differences in sediment fluxes throughout these two stations result from slightly higher SSC in the Tien River compared to the Hau River (presented in Fig. 5). The ratio of sediment fluxes between both stations is equivalent to recent studies (e.g. Dang et al., 2018; Manh et al., 2014), but magnitudes of sediment fluxes are somewhat lower. The lower sediment fluxes may come from a different period in estimation as we considered sediment fluxes in the low-flow season 2012 while Dang et al. and Manh et al. considered the low-flow season 2011. Dang et al. (2018) estimated that the sediment fluxes in 2011 at My Thuan (38.3 Mt) and Can Tho (23.4 Mt). These values are reliable because they are derived from daily measured data.

At the river mouths, the Mekong River delivers an amount of 22.8 Mt

to the sea in which it transports 10.7 Mt and 12.1 Mt, respectively, through the Tien and Hau branches. The Hau branch exports about 8.8 Mt and 3.3 Mt via the Dinh An and Tran De mouths respectively. Besides, the Tien River transports approximately 10.7 Mt of sediment by the Cung Hau (3.3 Mt), Co Chien (2.8 Mt), Ham Luong (1.3 Mt), Dai (1.9 Mt), and Tieu (1.4 Mt) mouths. Although water volume discharged by the Tien River's mouths is slightly higher than that by the Hau River's mouths (Thanh et al., 2020a), suspended sediment exported through the Tien River is smaller than the Hau River. This can be explained by the Tien River has larger depositional plains compared to the Hau River. This is determined by sediment deposition of about 18 Mt and 8 Mt from My Thuan (the Tien River) and Can Tho (the Hau River) to the coast, respectively. Previous studies did not directly compute sediment fluxes at the river mouths of the Mekong River, but computed transports at other stations on the mainstreams or extrapolate measured data (Dang et al., 2018; Nowacki et al., 2015). It was assumed that all sediment of the Mekong River would be transported to the sea. This study included riverbed deposition and erosion processes throughout the entire Mekong Delta for the first time.

Riverbed sediment exchange is difficult to measure especially throughout such a large domain. Our model suggests that riverbed erosion occurs in Cambodia while deposition happens in Vietnam. Unfortunately, observed data of riverbed change are unavailable to validate these results. They are also strongly affected by human activities, such as sand mining. Sand mining is probably much higher than the sedimentation rate of the Mekong River in Vietnam (Brunier et al., 2014). Moreover, estimated sand mining in the Hau River is about 7.75 million m³ in 2011 (Bravard et al., 2013) (~12.4 Mt, based on a bulk density of 1600 kg/m³) which is about one-third of the sedimentation rate of about 39.6 Mt. The sediment dynamics at the river mouths have seasonal variations. During the high flow season, the Mekong River supplies a substantial amount of sediment to the sea due to seaward residual velocity. During the low flow season, the tidal processes cause a small amount of landward sediment import (Gugliotta et al., 2017; Nowacki et al., 2015; Xing et al., 2017). The landward residual sediment flux has resulted from baroclinic effects (Nowacki et al., 2015). The modeled sediment fluxes at the river mouth stations capture characteristics of sediment exchange due to tidal processes.

Compared to other deltas over the world, sediment yield of the Mekong River is approximately equal to that of the Yangtze and twice higher than that of the Mississippi while the Mekong River catchment is smaller (Liu et al., 2009). Similarly, the annual sediment flux of these deltas is subject to human activities, such as hydropower dam construction and sand mining. The annual sediment flux of the Mekong River, the Yangtze and the Mississippi have recently reduced by 74%, 76%, and 55%, respectively (Binh et al., 2020; Yang et al., 2021).

Results of sediment budget are crucial in sediment management that quantify the balance between sediment inputs and outputs in the VMD. Understanding this balance helps managers make informed decisions about managing sand mining activities because the VMD is facing challenges due to sediment starvations. The sediment was decreased by 74.1% (Binh et al., 2020) caused by the compound impact of hydropower dams. The output of sediment budget enables more effective planning of interventions, adaptive strategies, protecting coastlines, ultimately leading to more sustainable management of sediment resources and coastal zones.

4.5. Limitations

This study investigates sediment dynamics and sediment budget in the Mekong Delta by using a process-based model. Reproducing sediment dynamics in the Mekong Delta remains a challenge due to limited data availability for calibration and validation. Although the study reproduces suspended sediment concentrations reasonably well, sediment transport measurements are rare, especially considering various sediment classes such as sand, silt and mud. More and more sophisticated

measurement campaigns are needed to further validate the model over the entire domain and during longer periods of time. These may include bathymetries, sediment transport loads, sediment properties and flow distribution over the VMD channel network. The VMD bathymetry has changed. Updating the bathymetry of the whole Mekong Delta is an extremely heavy work and this could consume some years. The only part of bathymetry updated was at the river mouths which was measured in 2016 (Thanh et al., 2017). In addition, our studies did not consider effects of both sand mining and hydropower dams. We first investigate the fate and transport of sediment, so these factors were excluded. For modeling sediment dynamics of the large-scale systems, single fraction of sediment can be used if it can reproduce 90% of the sediment budget (Achete et al., 2015). In addition, we only consider suspended sediment dynamics while other types of transport were neglected since the suspended sediment load contribute up to 97% of the total sediment load (Koehnken, 2012). The sediment budget of different years was included in the revised manuscript.

5. Conclusions

Historical measurements of suspended sediment entering the Mekong Delta reveal that the annual sediment loads are notably lower than the widely accepted estimate of 160 million tons. The quantity of suspended sediment transported annually exhibits significant variability, correlating closely with water discharge volumes. For example, measurements from 2011, which was a high-water year, indicate the Mekong River only carried a low amount of suspended sediment to its delta. This suggests the long-held 160 million ton per year estimate significantly overstates the true contemporary sediment supply to the Mekong Delta.

We used a 1D-2D numerical model to simulate the hydrodynamics and suspended sediment transport throughout the Mekong Delta, forced by rivers, tides and waves. The modeling grid covers the entire Mekong Delta, the connected Tonle Sap Lake, and its shelf. This grid considers the interaction between the Mekong River and the sea. In addition, the grid includes a dense network of rivers and man-made canals, considering hydrodynamics and sedimentation in the floodplain regions. Our modeling effort reproduces the hydrodynamics and SSC and transport. In sediment modeling, the erosion rate is an important parameter when considering bed-sediment availability.

This is one of the first studies which are able to investigate sediment dynamics at a large scale of the entire Mekong Delta. The model reproduces the suspended sediment concentrations and sediment fluxes at several stations located in different hydrological regions. Apart from changes in sediment availability in the bed we found that another cause of SSC hysteresis effect is the efficient sediment trapping by the Tonle Sap Lake. The inflow of the Tonle Sap Lake has a higher suspended sediment concentration compared to the outflow, causing clockwise

Appendix

loops of the hysteresis effects.

Our study confirms that the annual sediment load of the Mekong River into its delta is much lower than the common estimate. About 79% of the annual sediment load is transported to the VMD, but only 23% of the total sediment is exported to the East Sea. This suggests that the trapping efficiency of the VMD system is generally high (~73%).

This study indicates that numerical models are useful and efficient tools to gain a better understanding of hydrodynamics and sediment transport in large-scale areas. They are more helpful in the cases of the high variability of channel widths and large spatial scales. Due to taking the dense network of rivers and canals onboard, the model is likely impossible to apply at long time scales, such as centuries.

The data in this study are not publicly available due to their copyright but are available from the corresponding author on reasonable request. The analysis codes are publicly accessible in Zenodo (<https://zenodo.org/records/14056618>).

CRediT authorship contribution statement

Vo Quoc Thanh: Conceptualization, Data curation, Formal analysis, Methodology, Validation, Visualization, Writing – original draft, Writing – review & editing. **Dano Roelvink:** Conceptualization, Supervision, Writing – original draft, Writing – review & editing. **Mick van der Wegen:** Conceptualization, Supervision, Writing – original draft, Writing – review & editing. **Johan Reynolds:** Formal analysis, Methodology, Software, Writing – original draft, Writing – review & editing. **Ad van der Spek:** Supervision, Writing – original draft, Writing – review & editing. **Giap Van Vinh:** Data curation, Formal analysis. **Vo Thi Phuong Linh:** Data curation, Formal analysis. **Le Xuan Tu:** Data curation, Formal analysis. **Nguyen Hieu Trung:** Conceptualization, Supervision, Writing – original draft.

Declaration of competing interest

The authors declare the following financial interests/personal relationships which may be considered as potential competing interests: Dano Roelvink reports financial support was provided by Office of Naval Research. Dano Roelvink reports a relationship with Office of Naval Research that includes: funding grants.

Acknowledgments

This project is part of the ONR Tropical Deltas DRI and is funded under grants N00014-12-1-0433 and N00014-15-1-2824. The authors would like to thank Mekong River Commission for providing the data. Simulations were carried out on the Dutch national e-infrastructure with the support of the SURF Cooperative.

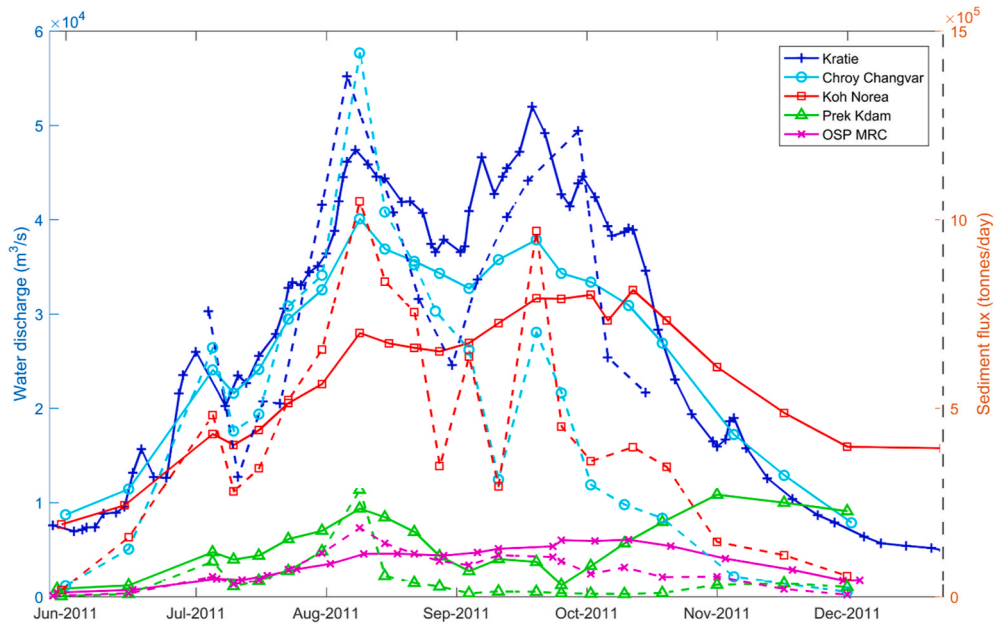


Fig. A1. Suspended sediment fluxes and water discharge on the main channels of the Mekong River in 2011 (aggregated from Koehnken, 2012). The dashed lines present sediment flux while the hatched lines show water discharge at the selected stations.

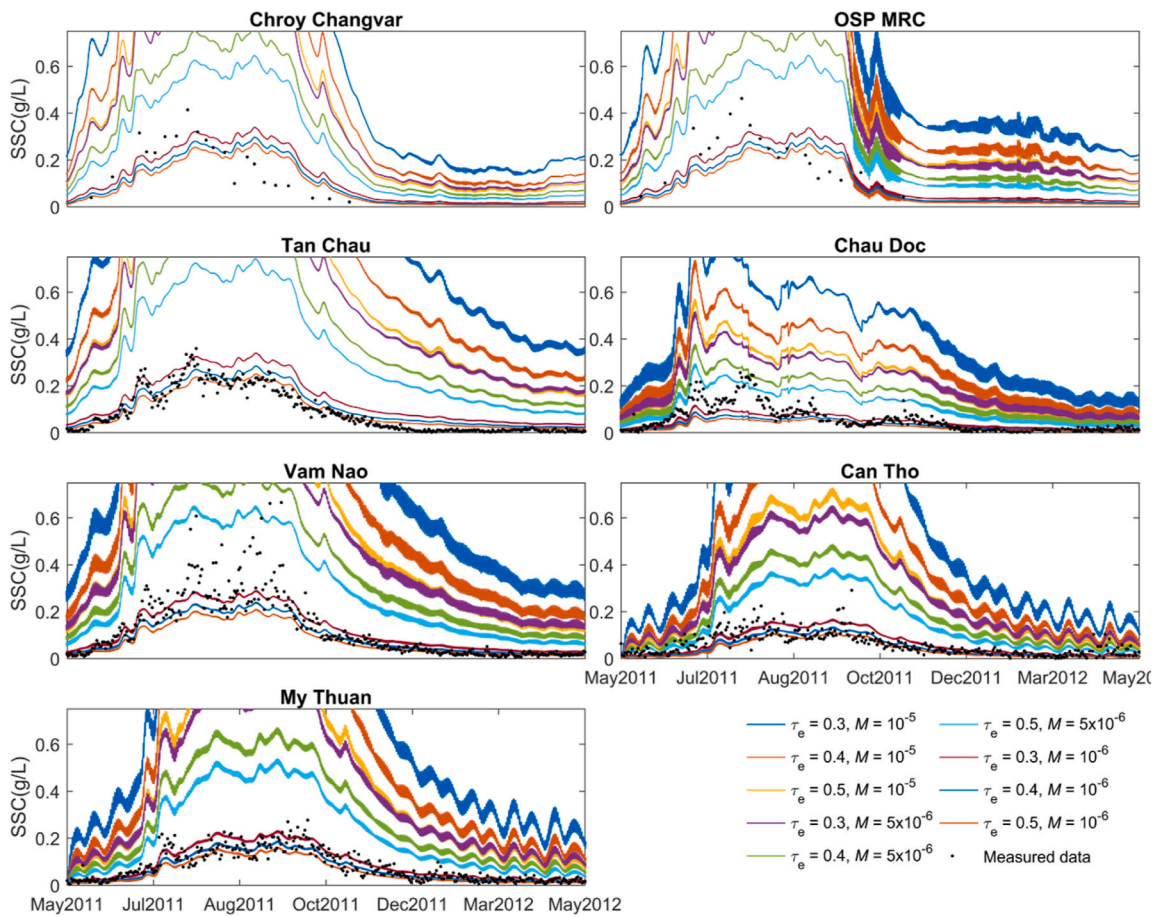


Fig. A2. Sensitivity analysis for SSC at the stations on the Mekong branch (right panels) and the Bassac branch (left panels).

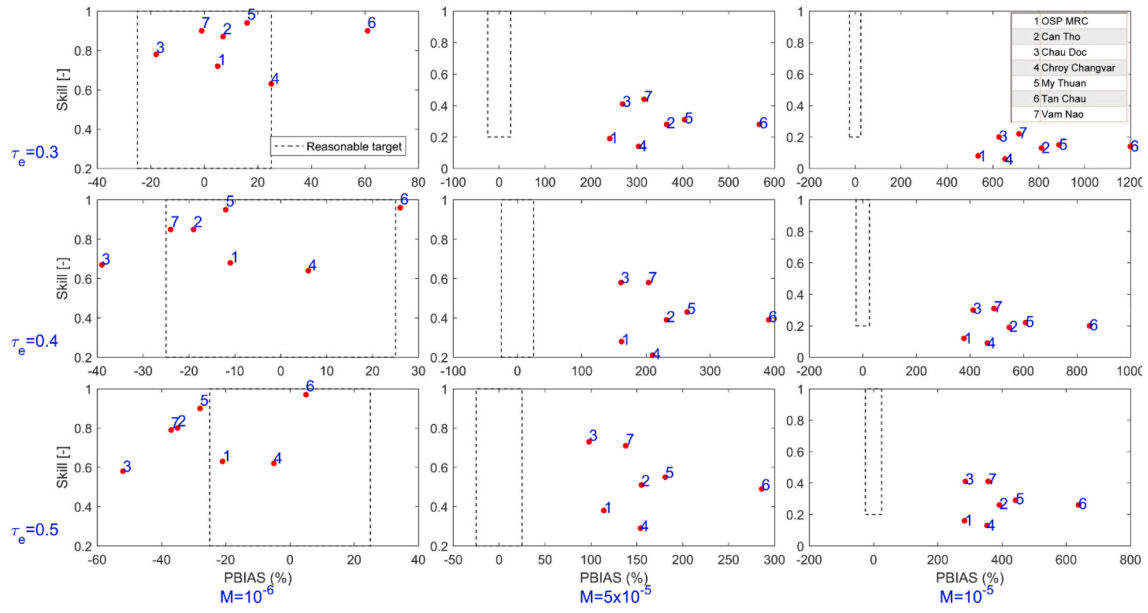


Fig. A3. Model performance of SSC in the sensitivity analysis. These simulations were set up with the same settling velocity, changing τ_{ce} and M parameters in the range presented in rows and columns, respectively. The target square presents the acceptable level of model performance. The locations of these stations are indicated in Fig. 1.

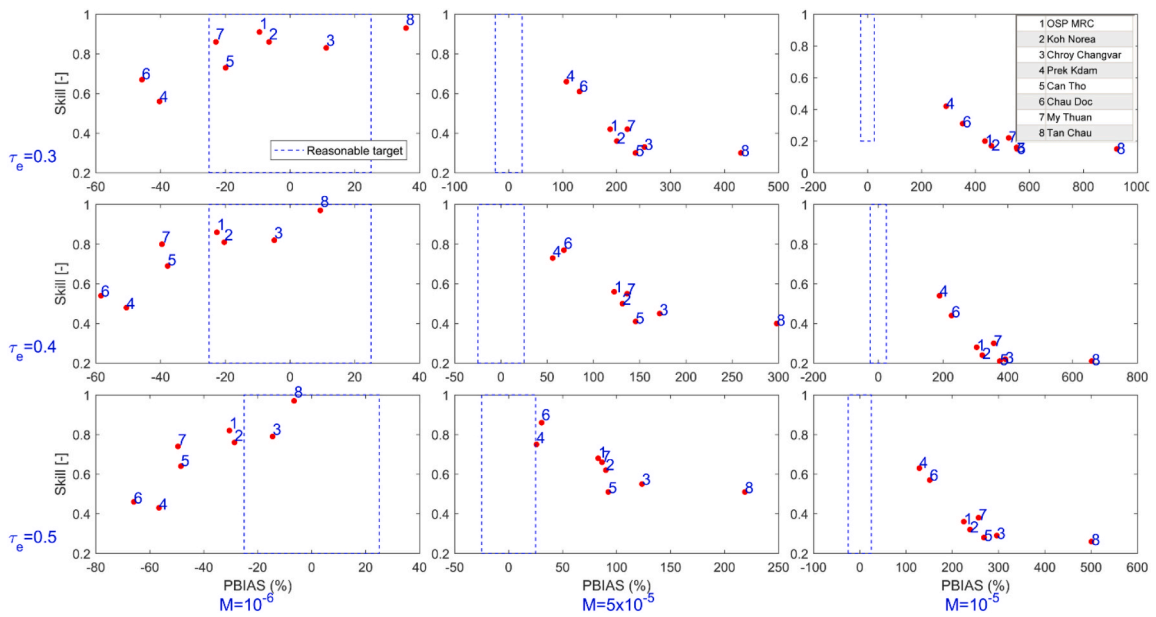


Fig. A4. Model performance of sediment fluxes in the sensitivity analysis. These simulations were set up with the same settling velocity, changing τ_{ce} and M parameters in the range presented in rows and columns, respectively. The target square presents the acceptable level of model performance. The locations of these stations are indicated in Fig. 1.

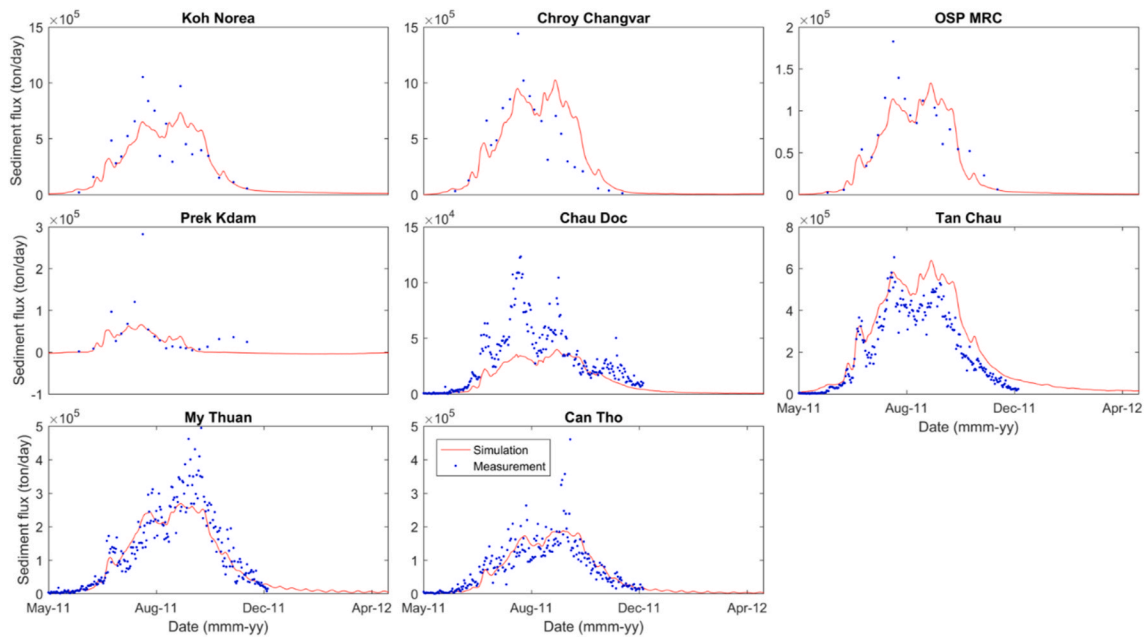


Fig. A5. Comparison of modeled and measured suspended sediment flux.

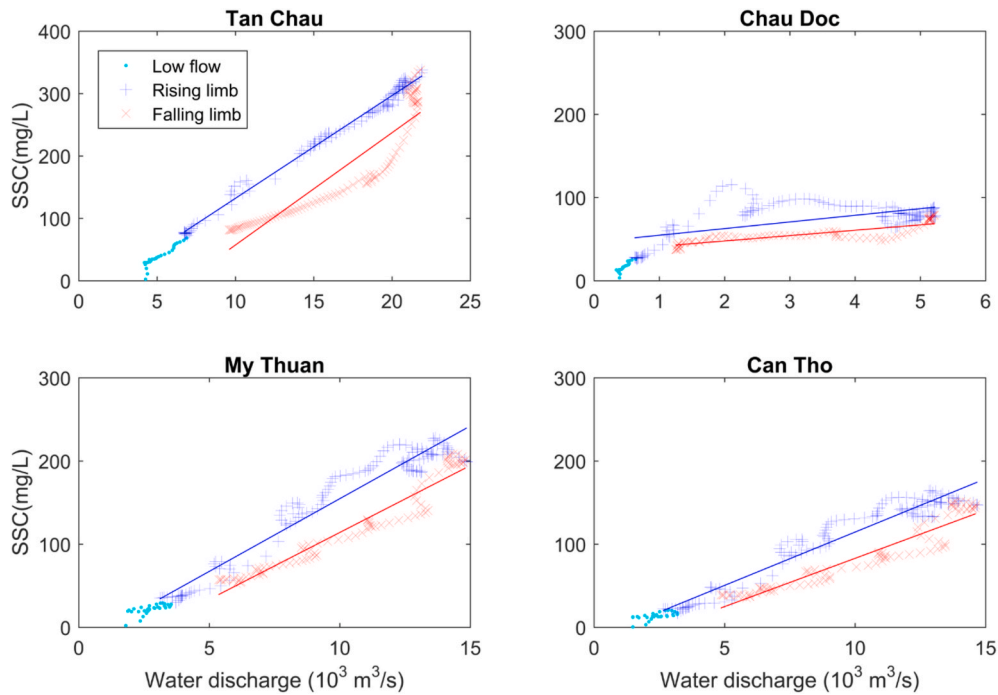


Fig. A6. Relationship between daily averaged modeled suspended-sediment concentration and water daily averaged discharge at four stations, namely Tan Chau, Chau Doc, My Thuan, and Can Tho. Low flow conditions are from January to June 2011. The rising phase begins from June to the yearly discharge peak in September, whereas the falling phase is taken from September to January 2011.

Data availability

Data will be made available on request.

References

Achete, F.M., van der Wegen, M., Roelvink, D., Jaffe, B., 2016. Suspended sediment dynamics in a tidal channel network under peak river flow. *Ocean Dynam.* 66, 703–718. <https://doi.org/10.1007/s10236-016-0944-0>.
 Achete, F.M., van der Wegen, M., Roelvink, D., Jaffe, B., 2015. A 2-D process-based model for suspended sediment dynamics: a first step towards ecological modeling.

Hydrol. Earth Syst. Sci. 19, 2837–2857. <https://doi.org/10.5194/hess-19-2837-2015>.
 ADB, 2013. *Climate Risks in the Mekong Delta: Ca Mau and Kien Giang Provinces of Viet Nam*.
 Anthony, E.J., Brunier, G., Besset, M., Goichot, M., Dussouillez, P., Nguyen, V.L., 2015. Linking rapid erosion of the Mekong River Delta to human activities. *Sci. Rep.* 5, 14745. <https://doi.org/10.1038/srep14745>.
 Berlamonta, J., Ockenden, M., Toormana, E., Winterwerp, J., 1993. The characterisation of cohesive sediment properties. *Coast. Eng.* 21, 105–128.
 Binh, D. Van, Kantoush, S., Sumi, T., 2020. Changes to long-term discharge and sediment loads in the Vietnamese Mekong Delta caused by upstream dams. *Geomorphology* 353, 107011. <https://doi.org/10.1016/j.geomorph.2019.107011>.

- Bravard, J.-P., Goichot, M., Gaillot, S., 2013. Geography of sand and gravel mining in the lower Mekong River. *EchoGéo* 0–20. <https://doi.org/10.4000/echogeo.13659>.
- Brunier, G., Anthony, E.J., Goichot, M., Provansal, M., Dussouillez, P., 2014. Recent morphological changes in the Mekong and Bassac river channels, Mekong delta: the marked impact of river-bed mining and implications for delta destabilisation. *Geomorphology* 224, 177–191. <https://doi.org/10.1016/j.geomorph.2014.07.009>.
- Chapman, A., Darby, S., 2016. Evaluating sustainable adaptation strategies for vulnerable mega-deltas using system dynamics modelling: rice agriculture in the Mekong Delta's an Giang Province, Vietnam. *Sci. Total Environ.* 559, 326–338. <https://doi.org/10.1016/j.scitotenv.2016.02.162>.
- Dang, T.H., Ouilillon, S., Vinh, G. Van, 2018. Water and suspended sediment budgets in the Lower Mekong from high-frequency. *Water* 10. <https://doi.org/10.3390/w10070846>.
- Darby, S.E., Hackney, C.R., Leyland, J., Kumm, M., Lauri, H., Parsons, D.R., Best, J.L., Nicholas, A.P., Aalto, R., 2016. Fluvial sediment supply to a mega-delta reduced by shifting tropical-cyclone activity. *Nat. Publ. Gr.* 539, 276–279. <https://doi.org/10.1038/nature19809>.
- Dartmouth Flood Observatory, 2004. Vietnam and Cambodia Lower Mekong: Rapid Response Inundation Map. *Deltares, 2020a. D-flow Flexible Mesh: User Manual. Delft, the Netherlands.*
- Deltares, 2020b. *Delft3D Flexible Mesh Suite: Technical Reference Manual.*
- Egbert, G.D., Erofeeva, S.Y., 2002. Efficient inverse modeling of barotropic ocean tides. *J. Atmos. Ocean. Technol.* 19, 183–204.
- Ferré, B., Sherwood, C.R., Wiberg, P.L., 2010. Sediment transport on the palos verdes shelf, California. *Continental Shelf Res.* 30, 761–780. <https://doi.org/10.1016/j.csr.2010.01.011>.
- Fujii, H., Garsdal, H., Ward, P., Ishii, M., Morishita, K., Boivin, T., 2003. Hydrological roles of the Cambodian floodplain of the Mekong River. *Int. J. River Basin Manag.* 1, 1–14. <https://doi.org/10.1080/15175124.2003.9635211>.
- Gibson, S., Comport, B., Corum, Z., 2017. Calibrating a sediment transport model through a gravel-sand transition: avoiding equifinality errors in HEC-RAS models of the Puyallup and White rivers. In: Dunn, C.N., Weele, B. Van (Eds.), *World Environmental and Water Resources Congress 2017. Sacramento, California*, pp. 179–191.
- Gratiot, N., Bildstein, A., Anh, T.T., Thoss, H., Denis, H., Michallet, H., Apel, H., 2017. Sediment flocculation in the Mekong River estuary, Vietnam, an important driver of geomorphological changes. *Compt. Rendus Geosci.* 349, 260–268. <https://doi.org/10.1016/j.crte.2017.09.012>.
- Gugliotta, M., Saito, Y., Van Lap, N., Thi Kim Oanh, T., Nakashima, R., Tamura, T., Uehara, K., Katsuki, K., Yamamoto, S., 2017. Process regime, salinity, morphological, and sedimentary trends along the fluvial to marine transition zone of the mixed-energy Mekong River delta, Vietnam. *Continental Shelf Res.* 147, 7–26.
- Gupta, A., Liew, S.C., 2007. The Mekong from satellite imagery: a quick look at a large river. *Geomorphology* 85, 259–274. <https://doi.org/10.1016/j.geomorph.2006.03.036>.
- Hoanh, C.T., Phong, N.D., Gowing, J.W., Tuong, T.P., Ngoc, N.V., Hien, N.X., 2009. Hydraulic and water quality modeling: a tool for managing land use conflicts in inland coastal zones. *Water Pol.* 11, 106–120. <https://doi.org/10.2166/wp.2009.107>.
- Hung, N.N., 2011. *Sediment Dynamics in the Floodplain of the Mekong Delta, Vietnam. Universität Stuttgart.*
- Hung, N.N., Delgado, J.M., Güntner, A., Merz, B., Bárdossy, A., Apel, H., 2014. Sedimentation in the floodplains of the Mekong delta, Vietnam Part II: deposition and erosion. *Hydrol. Process.* 28, 3145–3160. <https://doi.org/10.1002/hyp.9855>.
- Ji, Z., 2017. Water quality and eutrophication. In: *Hydrodynamics and Water Quality: Modeling Rivers, Lakes, and Estuaries. John Wiley & Sons Inc.*
- Kakonen, M., 2008. Mekong Delta at the crossroads: more control or adaptation? *Ambio* 37, 205–212.
- Kernkamp, H.W.J., Van Dam, A., Stelling, G.S., De Goede, E.D., 2011. Efficient scheme for the shallow water equations on unstructured grids with application to the continental shelf. *Ocean Dynam.* 61, 1175–1188. <https://doi.org/10.1007/s10236-011-0423-6>.
- Koehnken, L., 2014. *Discharge Sediment Monitoring Project (DSMP) 2009 – 2013 Summary & Analysis of Results. Mekong River Commission.*
- Koehnken, L., 2012. *IKMP discharge and sediment monitoring program review, recommendations and data analysis. Part 2: Data Analysis of Preliminary Results. Mekong River Commission, Phnom Penh, Cambodia.*
- Kumm, M., Penny, D., Sarkkula, J., Koponen, J., 2008. Sediment: curse or blessing for Tonle Sap Lake? *Ambio* 37, 158–163. [https://doi.org/10.1579/0044-7447\(2008\)37\[158:scobft\]2.0.co;2](https://doi.org/10.1579/0044-7447(2008)37[158:scobft]2.0.co;2).
- Kumm, M., Tes, S., Yin, S., Adamson, P., Józsa, J., Koponen, J., Richey, J., Sarkkula, J., Józsa, J., Koponen, J., Richey, J., Sarkkula, J., 2014. Water balance analysis for the Tonle Sap Lake-floodplain system. *Hydrol. Process.* 28, 1722–1733. <https://doi.org/10.1002/hyp.9718>.
- Kumm, M., Varis, O., 2007. Sediment-related impacts due to upstream reservoir trapping, the Lower Mekong River. *Geomorphology* 85, 275–293. <https://doi.org/10.1016/j.geomorph.2006.03.024>.
- Landers, M.N., Sturm, T.W., 2013. Hysteresis in suspended sediment to turbidity relations due to changing particle size distributions. *Water Resour. Res.* 49, 5487–5500.
- Lauri, H., de Moel, H., Ward, P.J., Räsänen, T.a., Keskinen, M., Kumm, M., 2012. Future changes in Mekong River hydrology: impact of climate change and reservoir operation on discharge. *Hydrol. Earth Syst. Sci.* 16, 4603–4619. <https://doi.org/10.5194/hess-16-4603-2012>.
- Le, H.-A., Gratiot, N., Santini, W., Ribolzi, O., Soares-Fraza, S., Deleersnijder, E., 2018. Sediment properties in the fluvial and estuarine environments of the Mekong River. In: *E3S Web of Conferences*, 05063. <https://doi.org/10.1051/e3sconf/20184005063>.
- Liu, J.P., Xue, Z., Ross, K., Wang, H.J., Yang, Z.S., Li, A.C., Gao, S., 2009. Fate of sediments delivered to the sea by Asian large rivers: long-distance transport and formation of remote alongshore clinothems. *Sediment. Rec.* 7, 4–9. <https://doi.org/10.2110/sedred.2009.4.4>.
- Lu, X., Kumm, M., Oeurng, C., 2014. Reappraisal of sediment dynamics in the lower Mekong River, Cambodia. *Earth Surf. Process. Landforms* 39, 1855–1865. <https://doi.org/10.1002/esp.3573>.
- Lu, X.X., Siew, R.Y., 2006. Water discharge and sediment flux changes in the Lower Mekong River. *Hydrol. Earth Syst. Sci.* 10, 181–195. <https://doi.org/10.5194/hessd-2-2287-2005>.
- Manh, N.V., Dung, N.V., Hung, N.N., Merz, B., Apel, H., 2014. Large-scale quantification of suspended sediment transport and deposition in the Mekong Delta. *Hydrol. Earth Syst. Sci.* 18, 3033–3053. <https://doi.org/10.5194/hessd-11-4311-2014>.
- Manh, N.V., Merz, B., Apel, H., 2013. Sedimentation monitoring including uncertainty analysis in complex floodplains: a case study in the Mekong Delta. *Hydrol. Earth Syst. Sci.* 17, 3039–3057. <https://doi.org/10.5194/hess-17-3039-2013>.
- Marchesiello, P., Nguyen, N.M., Gratiot, N., Loisel, H., Anthony, E.J., Dinh, C.S., Nguyen, T., Almar, R., Kestenare, E., 2019. Erosion of the coastal Mekong delta: assessing natural against man induced processes. *Continental Shelf Res.* 181, 72–89. <https://doi.org/10.1016/j.csr.2019.05.004>.
- Martyr-Koller, R.C., Kernkamp, H., van Dam, A., van der Wegen, M., Lucas, L.V., Knowles, N., Jaffee, B., Fregoso, T.A., 2017. Application of an unstructured 3D finite volume numerical model for hydrodynamic and water-quality transport in the San Francisco Bay-Delta system. *Estuar. Coast Shelf Sci.* 192, 86–107. <https://doi.org/10.1016/j.ecss.2017.04.024>.
- Mclachlan, R., Ogston, A., Allison, M., 2017. Implications of tidally varying bed shear stress and intermittent estuarine stratification on fine-sediment dynamics through the Mekong's tidal river to estuarine reach. *Continental Shelf Res.* 147, 27–37.
- Mekong River Commission, 2010. *State of the Basin Report 2010. Vientiane, Laos. ISSN:1728:3248.*
- Mhahshah, A., Bockelmann-Evans, B., Pan, S., 2018. Effect of hydrodynamics factors on sediment flocculation processes in estuaries. *J. Soils Sediments* 18, 3094–3103. <https://doi.org/10.1007/s11368-017-1837-7>.
- Milliman, J.D., Syvitski, J.P.M., 1992. Geomorphic/tectonic control of sediment discharge to the ocean: the importance of small mountainous rivers. *J. Geol.* 100 (5), 525–544. <https://doi.org/10.1086/629606>.
- Moriasi, D.N., Arnold, J.G., Van Liew, M.W., Bingner, R.L., Harmel, R.D., Veith, T.L., 2007. Model evaluation guidelines for systematic quantification of accuracy in watershed simulations. *Trans. ASABE (Am. Soc. Agric. Biol. Eng.)* 50, 885–900. <https://doi.org/10.13031/2013.23153>.
- MRC, 2005. *Overview of the Hydrology of the Mekong Basin. Mekong River Commission, Vientiane, Laos, 1728.3248.*
- Nguyen, a.D., Savenije, H.H.G., 2006. Salt intrusion in multi-channel estuaries: a case study in the Mekong Delta, Vietnam. *Hydrol. Earth Syst. Sci. Discuss.* 3, 499–527. <https://doi.org/10.5194/hessd-3-499-2006>.
- Nowacki, D.J., Ogston, A.S., Nittrouer, C.A., Fricke, A.T., Van, D.T.P., 2015. Sediment dynamics in the lower Mekong River: transition from tidal river to estuary. *J. Geophys. Res. Ocean.* 120. <https://doi.org/10.1002/2014JC010632>.
- Ogston, A.S., Allison, M.A., Mullarney, J.C., Nittrouer, C.A., 2017. Sediment- and hydrodynamics of the Mekong Delta: from tidal river to continental shelf. *Continental Shelf Res.* 147, 1–6. <https://doi.org/10.1016/j.csr.2017.08.022>.
- Partheniades, E., 1965. Erosion and deposition of cohesive soils. *J. Hydraul. Div.* 91, 105–139.
- Portela, L.L., Ramos, S., Teixeira, A.T., 2013. Effect of salinity on the settling velocity of fine sediments of a harbour basin. *J. Coast Res.* 1, 1188–1193. <https://doi.org/10.2112/SI65-201>.
- Renaud, F.G., Syvitski, J.P.M., Sebesvari, Z., Werners, S.E., Kremer, H., Kuenzer, C., Ramesh, R., Jenken, A.D., Friedrich, J., 2013. Tipping from the Holocene to the Anthropocene: how threatened are major world deltas? *Curr. Opin. Environ. Sustain.* 5, 644–654. <https://doi.org/10.1016/j.cosust.2013.11.007>.
- Roelvink, D., Walstra, D.-J., 2004. Keep it simple by using complex models. *Adv. hydro-science -engineering VI* 1–11.
- Sarkkula, J., Koponen, J., Lauri, H., Virtanen, M., 2010. *Origin, Fate and Impacts of the Mekong Sediments. Mekong River Commission.*
- Syvitski, J.P.M., Kettner, A., 2011. Sediment flux and the anthropocene. *Philos. Trans. R. Soc. A Math. Phys. Eng. Sci.* 369, 957–975. <https://doi.org/10.1098/rsta.2010.0329>.
- Talley, L.D., Pickard, G.L., Emery, W.J., Swift, J.H., 2011. *Dynamical processes for descriptive ocean circulation. In: Descriptive Physical Oceanography: an Introduction*, pp. 187–221. <https://doi.org/10.1016/b978-0-7506-4552-2.10007-1>.
- Thanh, V.Q., Reynolds, J., Wackerman, C., Eidam, E.F., Roelvink, D., 2017. Modelling suspended sediment dynamics on the subaqueous delta of the Mekong River. *Continental Shelf Res.* 147, 213–230. <https://doi.org/10.1016/j.csr.2017.07.013>.
- Thanh, V.Q., Roelvink, D., van Der Wegen, M., Reynolds, J., Kernkamp, H., Vinh, G. Van, Linh, V.T.P., 2020a. Flooding in the Mekong Delta: the impact of dyke systems on downstream hydrodynamics. *Hydrol. Earth Syst. Sci.* 24, 189–212.
- Thanh, V.Q., Roelvink, D., van der Wegen, M., Tu, L.X., Reynolds, J., Linh, V.T.P., 2020b. Spatial topographic interpolation for meandering channels. *J. Waterw. Port, Coast. Ocean Eng.* 146, 04020024.
- Tran, D.D., van Halsema, G., Hellegers, P.J.G.J., Phi Hoang, L., Quang Tran, T., Kumm, M., Ludwig, F., 2018. Assessing impacts of dike construction on the flood dynamics in the Mekong Delta. *Hydrol. Earth Syst. Sci. Discuss.* 22, 1875–1896. <https://doi.org/10.5194/hess-2017-141>.
- Tu, L.X., Thanh, V.Q., Reynolds, J., Van, S.P., Anh, D.T., Dang, T.D., Roelvink, D., 2019. Sediment transport and morphodynamical modeling on the estuaries and coastal

- zone of the Vietnamese Mekong Delta. *Continent. Shelf Res.* 186, 64–76. <https://doi.org/10.1016/j.csr.2019.07.015>.
- Unverricht, D., Szczuciński, W., Stattegger, K., Jagodziński, R., Le, X.T., Kwong, L.L.W., 2013. Modern sedimentation and morphology of the subaqueous Mekong delta, southern Vietnam. *Global Planet. Change* 110, 223–235. <https://doi.org/10.1016/j.gloplacha.2012.12.009>.
- van Kessel, T., Vanlede, J., de Kok, J., 2011. Development of a mud transport model for the Scheldt estuary. *Continent. Shelf Res.* 31, S165–S181. <https://doi.org/10.1016/j.csr.2010.12.006>.
- Van Liew, M.W., Veith, T.L., Bosch, D.D., Arnold, J.G., 2007. Suitability of SWAT for the conservation effects assessment project: comparison on USDA agricultural research service watersheds. *J. Hydrol. Eng.* 12, 173–189. <https://doi.org/10.1016/j.lwt.2017.04.076>.
- van Maren, D.S., Cronin, K., 2016. Uncertainty in complex three-dimensional sediment transport models: equifinality in a model application of the Ems Estuary, The Netherlands. *Ocean Dynam.* 66, 1665–1679. <https://doi.org/10.1007/s10236-016-1000-9>.
- Van, P.D.T., Popescu, I., Van Griensven, A., Solomatine, D.P., Trung, N.H., Green, A., 2012. A study of the climate change impacts on fluvial flood propagation in the Vietnamese Mekong Delta. *Hydrol. Earth Syst. Sci.* 16, 4637–4649. <https://doi.org/10.5194/hess-16-4637-2012>.
- Vinh, V.D., Ouillon, S., Van Thao, N., Ngoc Tien, N., 2016. Numerical simulations of suspended sediment dynamics due to seasonal forcing in the Mekong coastal area. *Water* 8, 255. <https://doi.org/10.3390/w8060255>.
- Vo, K.T., 2012. Hydrology and hydraulic infrastructure systems in the Mekong delta, Vietnam. In: Renaud, F., Kuenzer, C. (Eds.), *The Mekong Delta System—Interdisciplinary Analyses of a River Delta*. Springer, Heidelberg, Germany, pp. 49–83.
- Walling, D.E., 2009. The sediment load of the Mekong River. In: *The Mekong: Biophysical Environment of an International River Basin*, pp. 113–142.
- Walling, D.E., 2008. The changing sediment load of the Mekong River. *Ambio* 37, 150–157.
- Williams, G.P., 1989. Sediment concentration versus water discharge during single hydrologic events in rivers. *J. Hydrol.* 111, 89–106. [https://doi.org/10.1016/0022-1694\(89\)90254-0](https://doi.org/10.1016/0022-1694(89)90254-0).
- Willmott, C.J., 1981. On the validation of models. *Phys. Geogr.* 2, 184–194. <https://doi.org/10.1080/02723646.1981.10642213>.
- Winterwerp, J.C., Manning, A.J., Martens, C., de Mulder, T., Vanlede, J., 2006. A heuristic formula for turbulence-induced flocculation of cohesive sediment. *Estuar. Coast Shelf Sci.* 68, 195–207. <https://doi.org/10.1016/j.ecss.2006.02.003>.
- Wolanski, E., Huan, N.N., Dao, L.T., Nhan, N.H., Thuy, N.N., 1996. Fine-sediment dynamics in the Mekong River estuary, Viet Nam. *Estuar. Coast Shelf Sci.* 43, 565–582.
- Wolanski, E., Nhan, N.H., Spagnol, S., 1998. Sediment dynamics during low flow conditions in the Mekong River estuary, Vietnam. *J. Coast Res.* 14, 472–482.
- Xing, F., Meselhe, E.A., Allison, M.A., Weathers, H.D., 2017. Analysis and numerical modeling of the flow and sand dynamics in the lower Song Hau channel, Mekong Delta. *Continent. Shelf Res.* 147, 62–77. <https://doi.org/10.1016/j.csr.2017.08.003>.
- Yang, H.F., Yang, S.L., Li, B.C., Wang, Y.P., Wang, J.Z., Zhang, Z.L., Xu, K.H., Huang, Y. G., Shi, B.W., Zhang, W.X., 2021. Different fates of the Yangtze and Mississippi deltaic wetlands under similar riverine sediment decline and sea-level rise. *Geomorphology* 381, 107646. <https://doi.org/10.1016/j.geomorph.2021.107646>.
- Yu, W., Kim, Y., Lee, D., Lee, G., 2018. Hydrological assessment of basin development scenarios: impacts on the Tonle Sap Lake in Cambodia. *Quat. Int.* 0–1. <https://doi.org/10.1016/j.quaint.2018.09.023>.